

Journal Pre-proofs

Research Article

## **Protective Effects of Mirazid on Gentamicin-induced Nephrotoxicity in Rats through Antioxidant, Anti-inflammatory, JNK1/ iNOS, and Apoptotic Pathways; Novel Mechanistic Insights**

Samar A. Antar, Ahmed A. Al-Karmalawy, Ahmed A. E. Mourad, Magda Mourad, Mennaallah Elbadry, Sameh Saber, and Ahmed E. Khodir

**DOI:** 10.34172/PS.2022.4

**Please cite this article as:** Antar SA, Al-Karmalawy AA, Mourad AAE, Mourad M, Elbadry M, Saber S, Khodir AE. Protective effects of mirazid on gentamicin-induced nephrotoxicity in rats through antioxidant, anti-inflammatory, JNK1/ iNOS, and apoptotic pathways; novel mechanistic insights. Pharm Sci. 2022. doi:10.34172/PS.2022.4

**Received Date:** 27 September 2021

**Accepted Date:** 27 January 2022

This is a PDF file of an article which was accepted for publication in Pharmaceutical Sciences. It is assigned to an issue after technical editing, formatting for publication and author proofing

# Protective Effects of Mirazid on Gentamicin-induced Nephrotoxicity in Rats through Antioxidant, Anti-inflammatory, JNK1/ iNOS, and Apoptotic Pathways; Novel Mechanistic Insights

Samar A.Antar <sup>1</sup>, Ahmed A. Al-Karmalawy <sup>2,\*</sup>, Ahmed A. E. Mourad <sup>3</sup>, Magda Mourad <sup>4</sup>,  
MennaallahElbadry<sup>4</sup>, Sameh Saber <sup>4</sup>, and Ahmed E.Khodir <sup>1,\*</sup>

<sup>1</sup> Department of Pharmacology and Biochemistry, Faculty of Pharmacy, Horus University-Egypt, New Damietta, 34518, Egypt.

<sup>2</sup> Department of Pharmaceutical Medicinal Chemistry, Faculty of Pharmacy, Horus University-Egypt, New Damietta, 34518, Egypt.

<sup>3</sup> Department of Pharmacology and Toxicology, Faculty of Pharmacy, Port-Said University, Port-said 42511, Egypt.

<sup>4</sup> Department of Pharmacology and Biochemistry, Faculty of Pharmacy, Delta University for science and technology, Gamasa 11152, Egypt.

## \*Corresponding authors:

Ahmed A. Al-Karmalawy: **Email:** [akarmalawy@horus.edu.eg](mailto:akarmalawy@horus.edu.eg)

Ahmed E.Khodir: **Email:** [akhodir@horus.edu.eg](mailto:akhodir@horus.edu.eg)

## Abstract

**Background:** As the use of Gentamicin became more widespread, the drug's harmful effects, particularly nephrotoxicity, became increasingly well-known. Antibacterial and anti-inflammatory properties have long been associated with Mirazid. The goal of this research was to find out more about frameworks for the protection of Mirazid against nephrotoxicity triggered by Gentamicin.

**Methods:** Three groups of albino male rats were created; the normal group received only saline. In the second group, nephrotoxicity was produced for 10 days with Gentamicin (100 mg/kg; i.p.). In the third group; Mirazid (10 mg/kg; p.o.) was administered for 10 days before receiving Gentamicin. This was done to investigate the kidney/body weight index, serum creatinine, urea, lactate dehydrogenase (LDH), malondialdehyde (MDA), and Glutathione (GSH) levels. Moreover, immunohistochemical staining was done to study Jun N- terminal kinase 1 (JNK1), inducible nitric

oxide synthase (iNOS), and caspase3 expressions along with histopathological changes. Additionally, a molecular docking study was performed for the seventeen isolated and identified compounds from myrrh, JNK1 is inhibited by an oleo-gum resin derived from the Commiphora species of plants (Burseraceae).

**Results:** The Gentamicin group showed an increase in kidney/body weight index, serum creatinine, urea, LDH, and MDA, while decreasing GSH levels. Furthermore, immunohistochemical staining revealed increased JNK1, iNOS, and caspase3 expressions along with histopathological changes. All of these indicators were significantly reduced by mirazid, which also restored oxidant/antioxidant hemostasis. Furthermore, the histological architecture of tissues has been significantly conserved. Concerning the docking study, the isolated compound (**12**) was found to be superior to the co-crystallized inhibitor (**18**) with a binding score of -7.19 kcal/mol compared to -6.95, respectively.

**Conclusion:** Mirazid was found to be a potential method for suppressing the nephrotoxicity caused by Gentamycin by inhibiting the JNK1/ iNOS pathways, therefore preserving kidney function. The antioxidant, anti-inflammatory, and anti-apoptotic properties of mirazid are thought to be responsible for its preventive efficacy.

**Keywords:** Gentamicin, Mirazid, Nephrotoxicity, *In vivo*, JNK1/ iNOS, Molecular docking.

## 1- Introduction

Aminoglycosides have long been linked to drug-induced nephrotoxicity, which is one of the most common side effects<sup>1</sup>. Nephrotoxicity triggered by Gentamicin involves pathological conditions, such as altered intraglomerular hemodynamics, the toxicity of tubular cells, and inflammation<sup>2</sup>. Due to the disruption of oxidant-antioxidant systems, toxicity is induced by the generation of free radicals and protein oxidation<sup>3, 4</sup>. The production of reactive oxygen species (ROS), as well as the activation of a number of inflammatory mediators, have all been associated with gentamicin-induced nephrotoxicity<sup>5</sup>.

Oxidative stress-induced by gentamicin plays a vital role in the activation of pro-inflammatory cytokines, including Jun N-terminal Kinase (JNK1) which leads to kidney damage. Free radicals stimulate glomerulus lipid peroxidation and influence the normal physiological function of renal tissues, contributing to metabolic disorders<sup>6</sup>. Renal inflammatory cascades, renal oxidative stress, and pathogenic signaling systems are all exacerbated in nephrotoxicity<sup>7</sup>. Previous studies have indicated that medications with significant antioxidant and anti-inflammatory cellular characteristics can be employed to combat Gentamicin's nephrotoxicity<sup>8-10</sup>.

As the inflammatory system becomes more activated, pro-inflammatory mediators such as chemokines and cytokines are released, resulting in inflammatory signals. These signals enable the body to recognize, destroy, and eliminate foreign objects, resulting in an effective acute inflammatory response<sup>11</sup>. Immune suppression and the onset of chronic inflammatory diseases can be caused by the inappropriate production of pro- or anti-inflammatory mediators. Tissue injury and degeneration are connected to inflammation over time. This has been recognized as a necessary condition for the start of numerous neurological, autoimmune, and malignant diseases<sup>12</sup>. Macrophages are crucial participants in the immune and inflammatory responses that occur during a host's defense. Once activated, they start producing cytokines, oxygen, and nitrogen species. This stimulation causes cytokines to be released and enzymes like inducible nitric oxide synthase (iNOS) to be produced<sup>13</sup>.

Mirazid, a drug that has been on the Egyptian market for over a decade, is made from (Arabian or Somali) myrrh, an oleo-gum resin derived from plants of the Commiphora species (Burseraceae)<sup>14</sup>. Because of its antimicrobial activity<sup>14</sup>, infections and inflammation are treated with Mirazid<sup>15</sup>. Also, it treated blood stagnation, inflammatory diseases, and reduced swelling and pain<sup>16</sup>. In clinical trials, some myrrh-based recipes were utilized as anticancer medicines in the treatment of liver, pancreatic, and nasopharyngeal malignancies and have shown adequate curative efficacy<sup>17, 18</sup>. Extracts of these plants' resinous exudates and/or their constituents showed analgesic<sup>19</sup> anti-

inflammatory<sup>20</sup>, lipid-lowering<sup>21</sup> neuroprotective, and antibacterial properties<sup>22</sup>. Mirazid's influence on mucus formation and up-regulation in sulfhydryl concentrations of nucleic acid, as well as its free radical-scavenging, thyroid-stimulating, and prostaglandin-inducing capabilities are hypothesized to play a role in the treatment of stomach ulcers<sup>23</sup>.

One of the most essential technologies for drug discovery is computational drug design and development is molecular docking<sup>24-30</sup>. It helps scientists to design new drugs, repurpose existing candidates, or study their mechanisms of action<sup>31-38</sup>. Molecular docking is a crucial tool in molecular biology and computer-aided drug design<sup>39-44</sup>. Its main goal is to predict the most important binding mode(s) of a ligand with a protein of known 3D structure. Successful docking uses a scoring function that correctly ranks candidate dockings<sup>45-49</sup>.

The study of ways to reduce the toxicity of aminoglycosides continues to pique clinical interest. As a result, the goal of this study was to see how Mirazid affected oxidative stress, inflammation, and apoptotic pathways in Gentamicin-induced nephrotoxicity.

## **2- Materials and methods**

### **2.1. Experimental animals**

In this investigation, twenty-four male rats (albino Wistar) weighing 190-220 g were employed. The rats were provided by the Modern Veterinary Office For Laboratory Animals (Cairo, Egypt). Rats were kept in a temperature-controlled environment (25°C) with a 12-hour light/dark cycle. Food and water were allowed ad libitum during the study period. Before the trial, the rats were given two weeks to acclimate in the laboratory. The protocol for the experiment was approved by the Research Ethics Committee, Faculty of Pharmacy, Delta University (FPD4 15/2018).

### **2.2. Drugs**

Gentamicin (Gentamicin Sulphate) vials were purchased from Sigma company, U.S.A. Gentamicin sulfate is 80 mg per ml in each vial. Mirazid capsules were purchased from the producing company Pharco Pharmaceuticals (Alexandria, Egypt).

### **2.3. Induction of nephrotoxicity**

The intraperitoneal administration of Gentamicin (100mg/kg/ body weight) for 10 days resulted in nephrotoxicity.<sup>50</sup>

### **2.4. Experimental protocols**

Twenty-four rats were allocated into three groups at random (8 rats each). Control group, rats did not receive any drug or solvent, Gentamicin group; rats were injected with Gentamicin (100

mg/kg;i.p.) for 10 days and Mirazid prophylactic group; Mirazid (10mg/kg;p.o.) was administrated to rats starting 10 days before Gentamicin administration<sup>50</sup>.

## **2.5. Sacrification and biological samples collection**

Under light ether anesthesia, a clean sterile capillary tube was inserted in the inner canthus of the eye to collect blood samples from the orbital sinus (retro-orbital plexus). After allowing the blood to coagulate for 20 minutes, it was centrifuged for 15 minutes at 4000 rpm. The serum samples were then separated, collected in clean tubes, and maintained at -20°C until they were used to determine serum creatinine, urea levels, and lactate dehydrogenase (LDH) levels using a colorimetric kit, as directed by the manufacturer. Rats were sedated with thiopental sodium (50 mg/kg) and killed by cervical dislocation at the end of the experiment. The kidneys were separated and rinsed in ice-cold phosphate-buffered saline (pH = 7.4). Body weights and kidney weights were measured for the calculation of kidney/body weight index. The right kidney was rinsed in ice-cold saline, sliced lengthwise, and preserved in 10% buffered formalin for histological investigation. The left kidney was submerged in liquid nitrogen and stored at 80 °C for tissue homogenate preparation.

## **2.6. Preparation of kidney homogenate**

Kidney homogenate (10% w/v) was made using roughly 2 cm of kidney tissue in ice-cold KCl (1.15 percent, pH 7.4). The homogenate was centrifuged for 10 minutes at 3000 rpm at 4 °C, and the supernatants were decanted and utilized to measure kidney GSH and MDA levels.

## **2.7. Determination of serum creatinine, urea, and lactate dehydrogenase (LDH)**

The assay is based on Jaffe's description of the reaction of creatinine with sodium picrate. Creatinine forms a crimson complex with alkaline picrate. Interferences from other serum constituents are avoided by the time interval used for measurements. The amount of colour generated is proportional to the amount of creatinine in the sample. Serum urea was determined enzymatically according to the previously described method of Kaplan and Kohn<sup>51</sup>. The level of LDH in the serum was determined using a spectrophotometer and commercially available kits (Biomed Diagnostics test kits), as directed by the manufacturer (Egypt).

## **2.8. Determination of kidney GSH concentration and MDA content**

GSH concentration and MDA content were determined according to the manufacturer's instructions using a commercially available kit (Biodiagnostic, Giza, Egypt). According to a previously established approach, lipid peroxidation (LPO) was measured as thiobarbituric acid reactive substances (TBARS) in terms of generated MDA<sup>52</sup>. Glutathione (GSH) content was assessed according to a method illustrated earlier<sup>53</sup>.

## **2.9. Histopathological examination**

For histological assessment, a 2 cm piece of the right kidney was removed, rinsed in cold saline, fixed in 10% buffered formalin solution, sliced transversely, paraffin-embedded, and 3mm slices stained with hematoxylin and eosin (H&E). The tissues were evaluated using an Olympus CX21 microscope in a random order, with the histopathologist blinded to the experimental groups. For image analysis, slides were taken using an Olympus® digital camera set on an Olympus® microscope with 1/2 X photo adapter and a 40 X objective utilizing a computer-assisted digital image analysis (Digital morphometric study). The photos were examined using Video Test Morphology® software (Russia) with a built-in process for stain quantification and automated object analysis on an Intel® Core I3® based computer. All measurements are validated against a micrometer slide that was photographed with the same instrument at the same magnification using the same technique. This allows measurements to be taken in  $\mu\text{m}^2$  rather than square pixels. SO for Hx, the change in the number of inflammatory cells ( $\text{cells}/\mu\text{m}^2$ ).

## **2.10. Immunohistochemical evaluation of JNK 1, iNOS and Caspase3**

For antigen retrieval, kidney slices were dewaxed and submerged in a solution of 0.05 M citrate buffer, pH 6.8. After that, the sections were treated with 0.3 % hydrogen peroxide and protein block. The sections were then treated with anti-JNK1, anti-iNOS, and anti-caspase3 polyclonal antibodies (Santa Cruz, Cat# (F-6): sc-8008, 1:100 dilution). After rinsing with phosphate-buffered saline, they were incubated for 30 minutes at room temperature with a goat anti-rabbit secondary antibody (Cat# K4003, EnVision+™ System Horseradish Peroxidase Labelled Polymer; Dako). Slides were visualized using a DAB kit before being counterstained with Mayer's hematoxylin. In a total of 1000 cells per 8 HPF, the staining intensity was evaluated and expressed as a percentage of positive expression. All measurements are calibrated against a micrometer slide that was photographed with the same instrument at the same magnification using the same technique. This allows measurements to be taken in  $\mu\text{m}^2$  rather than square pixels. JNK 1, iNOS, and Caspase-3 are scored based on the change in staining intensity.

## 2.11. Docking studies

Using GC–MS, and ICP–MS separation techniques, we previously identified seventeen chemicals from myrrh resin<sup>54</sup> that were subjected to molecular docking studies using MOE 2019.012 suite<sup>55, 56</sup> to propose its mechanism of action as a promising JNK-1 inhibitor. JNK-1 inhibition is responsible for stopping both the apoptotic and iNOS pathways which are proposed to be the main mechanism of action responsible for the anti-inflammatory effects of myrrh. Also, thiophenecarboxamide urea (TCU) native co-crystallized inhibitor was used as a reference standard.

### 2.11.1. Preparation of the myrrh resin extract

The seventeen isolated and identified compounds from myrrh resin were downloaded from the PubChem database website. They were inserted into MOE and prepared for docking by applying the previously described steps<sup>57-59</sup>. Then, they were imported together with the co-crystallized JNK-inhibitor (TCU) in a single database file and saved as an MDB file to be ready for the docking process.

### 2.11.2. Preparation of the target JNK-1 pocket

The JNK-1 X-ray structure (code: [3PZE](#))<sup>60</sup> was downloaded from the Protein Data Bank and the full preparation steps for its preparation were applied as before<sup>61-64</sup>.

### 2.11.3. Docking of myrrh isolated compounds to the binding pocket of JNK-1

The prepared database containing the isolated identified compounds was inserted in a general docking process and all the default methodology steps were performed as described earlier<sup>65-68</sup>. By the end, we filtered the best poses according to their scores, RMSD, and amino acid interactions for all the examined compounds. Moreover, a process of redocking for the co-crystallized ligand inside the binding pocket of the JNK-1 receptor was applied to validate the MOE program. The validation was confirmed by obtaining low RMSD values (< 1) between the docked and native ligands<sup>69-72</sup>.

## 2.12. Statistical analysis

For statistical comparison between parametric and nonparametric data, one-way analysis of variance (ANOVA) followed by Tukey–Kramer multiple comparison tests and Kruskal-Wallis test followed by Dunn's Multiple Comparison tests were employed, respectively. A *P*-value < 0.05 was the established level of significance

## 3- Results

### 3.1. Effect of prophylactic Mirazid on Gentamicin triggered a modification in the serum level of creatinine, urea levels, and LDH



When compared to the control group, serum creatinine and urea levels were considerably ( $P < 0.05$ ) higher following Gentamicin administration. Prophylactic daily oral Mirazid (10 mg/kg) for 10 days resulted in a substantial ( $P < 0.05$ ) decrease in serum creatinine and BUN as compared to the Gentamicin group. The nephrotoxicity marker LDH is used to diagnose renal impairment. Gentamicin treatment greatly deteriorated kidney functions contrasted to the control group. Serum LDH levels increased significantly ( $P < 0.05$ ). Prophylactic daily oral Mirazid (10 mg/kg) for 10 days resulted in a substantial ( $P < 0.05$ ) decrease in serum LDH as compared to the Gentamicin group (**Table 1**).

**Table 1.** Effect of Mirazid (10mg/kg;p.o) on Gentamycin (100 mg/kg; i.p.) triggered a modification in serum creatinine, BUN, and LDH.

| Treatment group            | Creatinine (mg/dl) | BUN (mmol/l)   | LDH (U/L)      |
|----------------------------|--------------------|----------------|----------------|
| Control                    | 0.32 ± 0.02        | 36.75± 1.8     | 1350 ± 19.5    |
| Gentamicin group           | 0.74 ± 0.01*       | 114.60 ± 3.1 * | 4409 ± 10.9 *  |
| Mirazid prophylactic group | 0.41 ± 0.01 #      | 41.33 ± 2.3 #  | 1675 ± 11.94 # |

Results are expressed as mean± S.E.M, n = 8. Statistical analysis was performed using One-Way ANOVA followed by Tukey-Kramer multiple comparisons test at  $P < 0.05$ . \* $P < 0.05$  concerning the control group, # $P < 0.05$  concerning the Gentamicin group.

### 3.2. Effect of prophylactic Mirazid on Gentamicin triggered a modification in oxidants/antioxidant stress markers in the kidney; MDA content and decreased GSH

The administration of gentamicin elevated MDA levels while lowering GSH levels significantly. Concurrent administration of Mirazid (10 mg/kg, orally) significantly ( $P < 0.05$ ) ameliorated Gentamicin-induced kidney damage. As MDA content was reduced and GSH activity was restored. Mirazid significantly preserved kidney GSH activity when contrasted to the Gentamicin group and significantly decreased kidney MDA activity in rats in comparison with the disease group. On the other hand, Gentamicin administration showed a significant ( $P < 0.05$ ) up-regulation in MDA activity when contrasted to the control group (**Table, 2**).

**Table 2.** Effect of Mirazid (10 mg/kg;p.o) on Gentamycin (100 mg/kg; i.p.) triggered a modify in kidney homogenate GSH and MDA concentration.

| Groups                     | GSH<br>( $\mu\text{mol/g tissue}$ ) | MDA<br>( $\text{nmol/g tissue}$ ) |
|----------------------------|-------------------------------------|-----------------------------------|
| Control                    | $0.71 \pm 0.02$                     | $33.75 \pm 1.8$                   |
| Gentamicin group           | $0.32 \pm 0.01$ *                   | $111.10 \pm 3.3$ *                |
| Mirazid prophylactic group | $0.69 \pm 0.04$ #                   | $48.33 \pm 2.3$ #                 |

Results are expressed as mean  $\pm$  S.E.M, n = 8. Statistical analysis was performed using One-Way ANOVA followed by Tukey-Kramer multiple comparisons test at  $P < 0.05$ . \* $P < 0.05$  concerning the control group, # $P < 0.05$  concerning the Gentamicin group.

### 3.3. Effect of prophylactic Mirazid on Gentamicin triggered a modification in kidney/body weight index

When compared to the control group, the kidney/body weight ratio of the Gentamicin group was considerably higher ( $P < 0.05$ ). The Mirazid prophylactic group, on the other hand, saw a significant ( $P < 0.05$ ) reduction in kidney weight when compared to the Gentamicin group. According to Mirazid prophylactic group, there was a significant improvement in modifying kidney/body weight index. However, the kidney/ body weight index of Mirazid prophylactic group is still significantly increasing in comparison to the control group; it could not reach normal weight (**Figure, 1**).

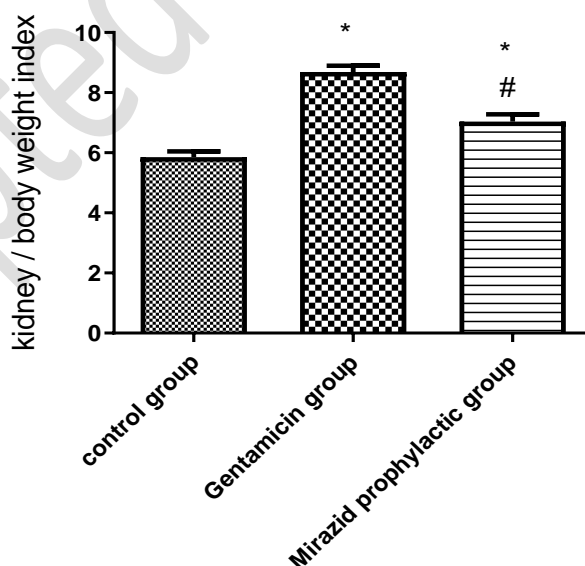


**Figure (1):** Effect of Mirazid (10mg/kg) orally for 7days on Gentamycin (100 mg/kg; I.P)-induced changes in kidney /body weight index. Results are expressed as mean  $\pm$  S.E.M, n = 8. Statistical analysis was performed using One-Way ANOVA followed by Tukey-Kramer multiple comparisons test at  $P < 0.05$ . \* $P < 0.05$  concerning the control group, # $P < 0.05$  concerning the Gentamicin group.

### 3.4. Effect of prophylactic Mirazid on hematoxylin and eosin-stained kidney specimens, gentamicin caused histopathological changes

As illustrated in Figure 2, kidney tissue photomicrographs of A, control animal showing normal glomeruli with an intact bowman's capsule (arrow); B, sections of animals treated with gentamycin showing glomerular congestion (arrow), inflammatory cell infiltration (filled arrowhead), and necrosis (open arrowhead); C, sections of animals exposed to gentamycin and treated with mirazid showed isolated mild tubular damage in the form of tubular dilatation with an irregular contour and tubular vacuolization (filled arrowhead), but no glomerular abnormalities or neutrophil infiltration were observed (arrow). Scale bar = 20  $\mu\text{m}$ .

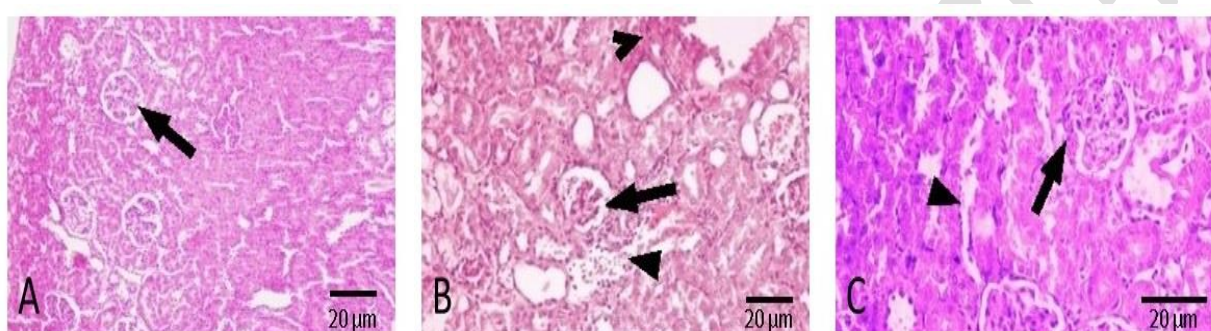


**Figure (2):** Representative photomicrographs for sections from renal tissue of rats stained with H&E stain. Scale bar = 20  $\mu\text{m}$ .

**Table 3.** Effect of Mirazid on Gentamicin (100 mg/kg; I.P)- triggered a modification in inflammatory cells count for H&E.

| Groups                     | Inflammatory cells<br>(cells / $\mu\text{m}^2$ ) |
|----------------------------|--|
| Control group              | 20.50 $\pm$ 1.11                                 |
| Gentamicin group           | 177.3 $\pm$ 6.33 *                               |
| Mirazid prophylactic group | 120.7 $\pm$ 5.01 *#                              |

Results are expressed as mean  $\pm$  S.E.M, n = 8. Statistical analysis was performed using One-Way ANOVA followed by Tukey-Kramer multiple comparisons test at  $P < 0.05$ . \* $P < 0.05$  concerning the control group, # $P < 0.05$  concerning the Gentamicin group.

### 3.5. Effect of prophylactic Mirazid on Gentamicin triggered activation of renal apoptosis; immunohistochemical analysis of caspase-3 expression

As an apoptotic marker, the expression of caspase 3 stained cells in tissue was evaluated. Caspase-3 immunostaining was negative in the control group. On the contrary, the Gentamicin group

showed strong immunostaining for caspase-3 indicating the existence of apoptotic activity in kidney tissue contrasted to the control group. Caspase-3 expression was downregulated in the prophylactic daily oral Mirazid (10 mg/kg) contrasted to the Gentamicin group (**Figure, 3**).

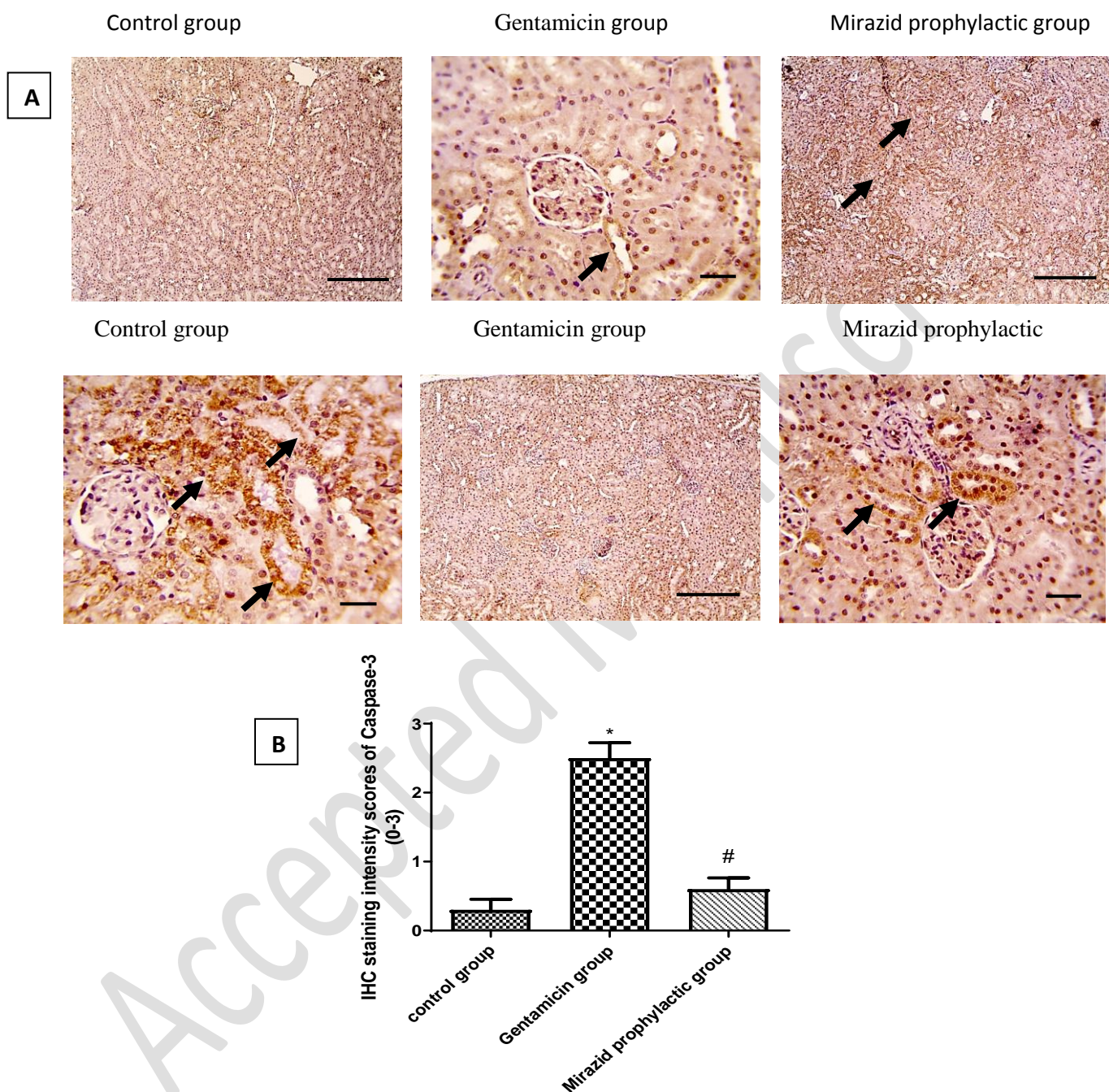


**Figure (3):** A) Microscopic pictures of immune-stained renal sections against Caspase3. IHC counterstained with Mayer's hematoxylin. Black arrows point to positive tubules. Low magnification X:100 bar 100 and high magnification X:400 bar 50 B). Effect of Mirazid (10 mg/kg) orally for 7days on Gentamycin (100 mg/kg; I.P)-induced change in inflammatory cells to count for H&E. Results are expressed as mean± S.E.M, n = 8. Statistical analysis was performed using One-Way ANOVA followed by Tukey-Kramer multiple comparisons test at  $P < 0.05$ . \* $P < 0.05$  concerning the control group, # $P < 0.05$  concerning the Gentamicin group

### 3.6. Effect of prophylactic Mirazid on Gentamicin triggered activation of renal inflammation; immunohistochemical analysis of i-NOS and JNK1 expressions

Expressions of i-NOS and JNK1 stained cells were evaluated as a marker of inflammation. The Control group revealed negative immunostaining for i-NOS (*Figure,4*) and JNK1 (*Figure,5*). The Gentamicin group showed strong immunostaining for i-NOS and JNK1 expressions contrasted to the control group. On the other hand, Prophylactic daily oral Mirazid (10 mg/kg) dose downregulated i-NOS and JNK1 expressions contrasted to Gentamicin group, yet this decrease failed to reach a normal level.

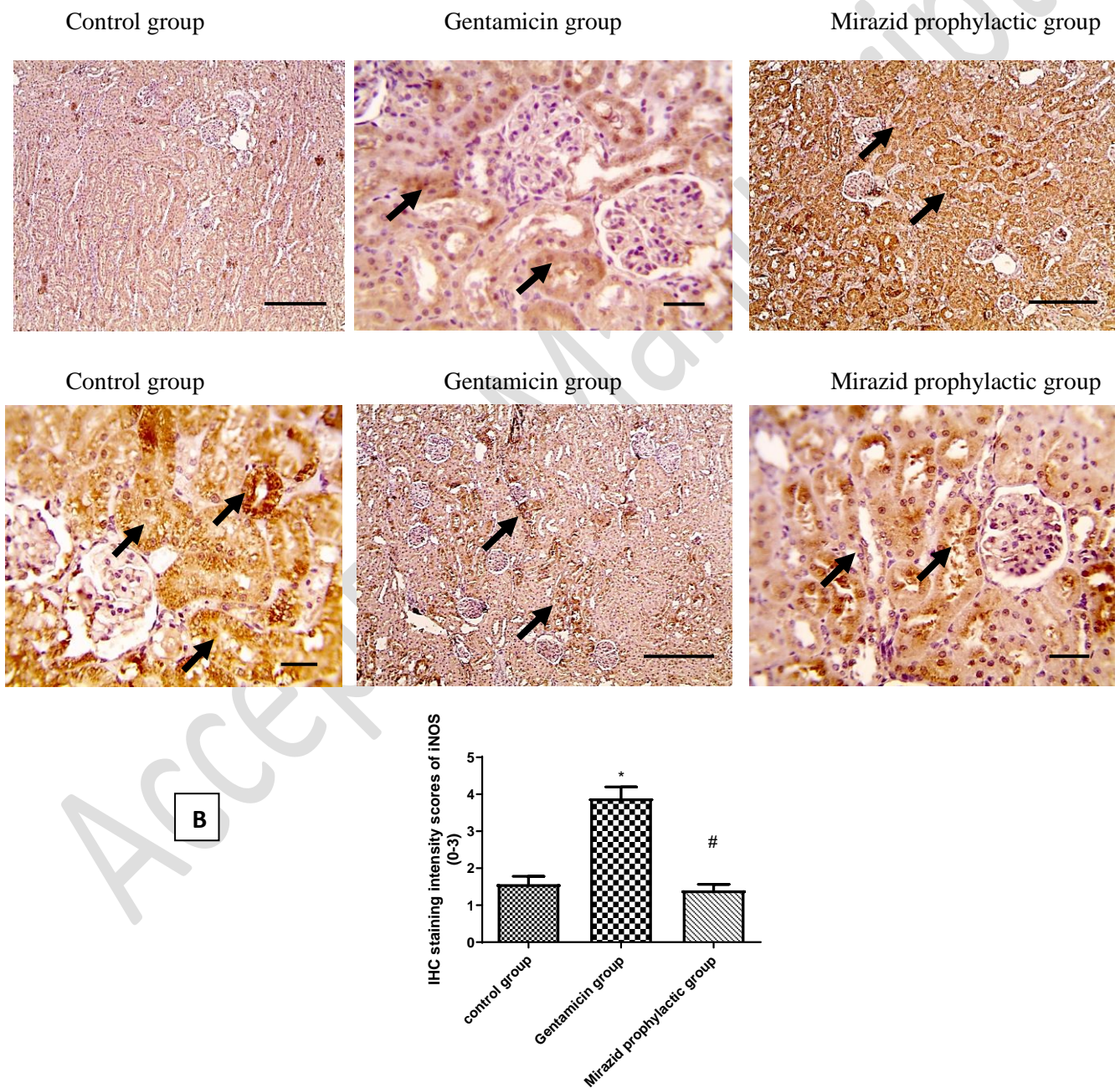


**Figure (4):** A) Microscopic pictures of immune-stained renal sections against iNOS. IHC counterstained with Mayer's hematoxylin. Black arrows point to positive tubules. Low magnification

X:100 bar 100 and high magnification X:400 bar 50 **B**) Effect of Mirazid (10 mg/kg) orally for 7dayson Gentamycin (100 mg/kg; I.P)-induced change in inflammatory cells to count for H&E. Results are expressed as mean± S.E.M, n = 8. Statistical analysis was performed using One-Way ANOVA followed by Tukey-Kramer multiple comparisons test at  $P < 0.05$ . \* $P < 0.05$  concerning the control group, # $P < 0.05$  concerning the Gentamicin group.

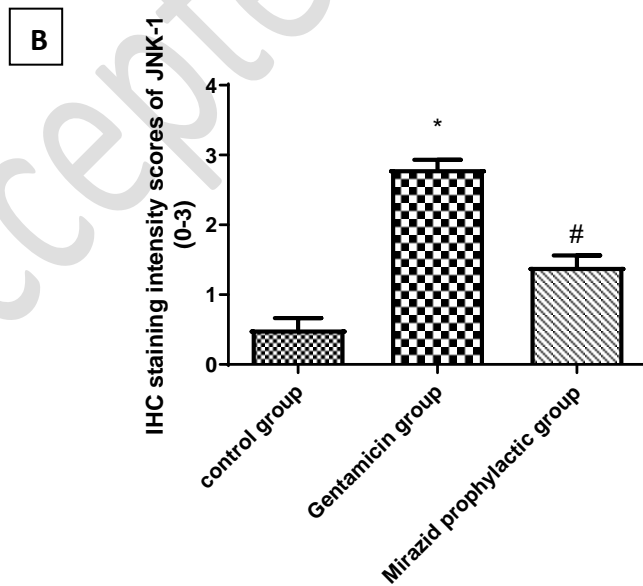
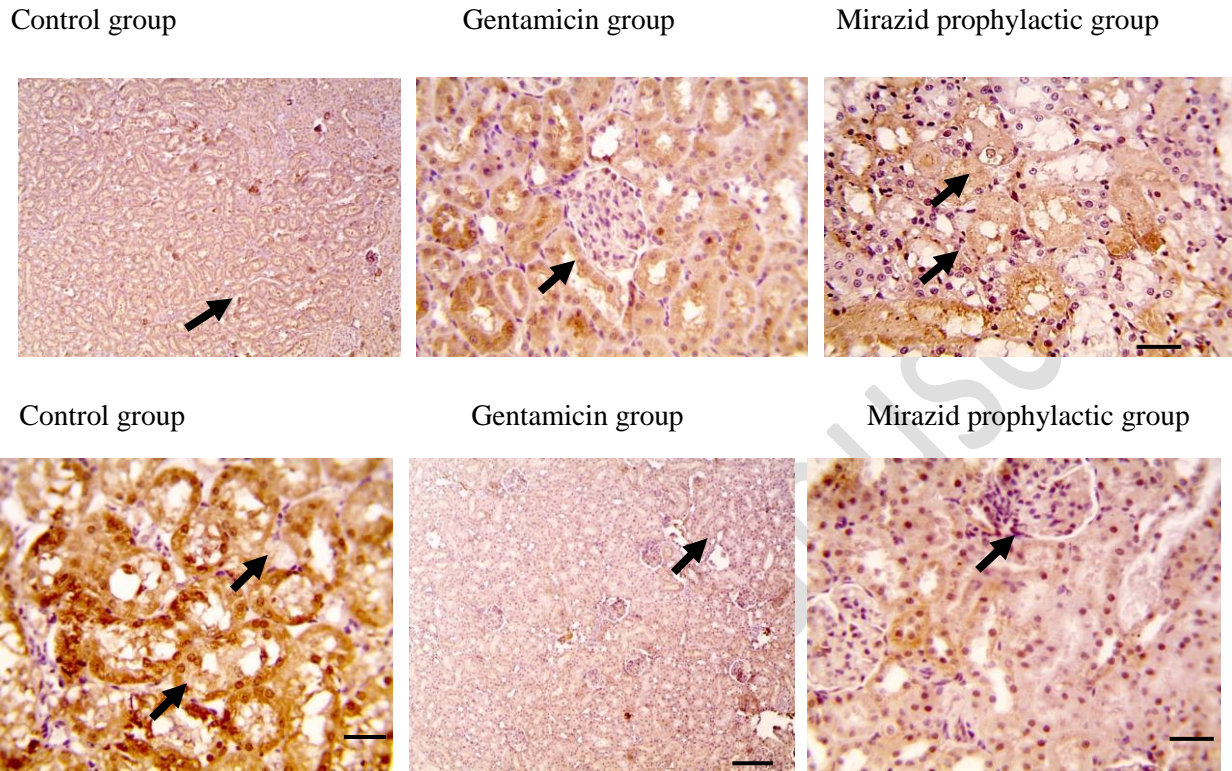


**Figure (5):** A) Microscopic pictures of immune-stained renal sections against JNK. IHC counterstained with Mayer's hematoxylin. Black arrows point to positive tubules. Low magnification X:100 bar 100 and high magnification X:400 bar 50 B) Effect of Mirazid (10 mg/kg) orally for 7 days on Gentamycin (100 mg/kg; I.P)-induced change in inflammatory cells to count for H&E. Results are expressed as mean± S.E.M, n = 8. Statistical analysis was performed using One-Way ANOVA followed by Tukey-Kramer multiple comparisons test at  $P < 0.05$ . \* $P < 0.05$  concerning the control group, # $P < 0.05$  concerning the Gentamicin group

### 3.7. Docking studies

Through the creation of five H-bonds with Met108, Glu109, and Met111 amino acids, the x-ray structure of JNK revealed the fitting of its co-crystallized inhibitor (TCU) inside its binding pocket. Also, it formed two extra H-bonds with Gln117 amino acid through an intermediate bridging H<sub>2</sub>O515 molecule. Molecular docking of the previously isolated compounds from myrrh resin compared to the docked co-crystallized inhibitor of JNK revealed the following descending binding order: oxalic acid, hexyl 2-methyl phenyl ester (**12**) > docked co-crystallized TCU inhibitor (**18**) > germacrene B (**4**) > (-)-elema-1,3,11(13)-trien-12-ol (**2**) > isoserinenine (**5**) > 3-[(E)-2-phenyl-1-propenyl]cyclohexanone (**6**) > 2,5,8-trimethyl-1-nonen-3-yn-5-ol (**7**) ≥ 2-(2-hydroxy-2-methyl-2-phenylethyl)-3-methyl (**14**) > curzerene (**3**) > beta selinene (**8**) > spathulenol (**9**) ≥ 1-deoxycapsidiol (**10**) > myrcenol (**15**) > (-)-caryophyllene oxide (**11**) > (-)-(R)-ipsdienol (**13**) > 2,8-decadiene (**16**) > R(+)-limonene (**1**) > bicyclo[3.1.1]hept-2-ene-2-carboxaldehyde,6,6-dimethyl-,(1S)- (**17**). Moreover, their binding scores and interactions with the amino acids of the JNK pocket are depicted in (**Table 4**) and **supplementary data**.

The findings of docking simulation showed that the docked co-crystallized TCU inhibitor (**18**) showed nearly the same binding mode of its native co-crystallized form, where it formed four H-bonds with Met108, Glu109, and Met111 amino acids. At the same time, it formed the two extra H-bonds with Gln117 amino acid through the intermediate bridging H<sub>2</sub>O515 molecule. Its binding score was found to be -6.95 kcal/mol and the RMSD value was 1.18. On the other hand, surprisingly, oxalic acid, hexyl 2-methyl phenyl ester (**12**) achieved a superior binding score (-7.19 kcal/mol) than the docked co-crystallized TCU inhibitor (**18**) with an RMSD value of 1.25. It got stabilized through the formation of only one H-bond with Asn114 amino acid which indicates a highly stabilized fitting of the molecule regardless of the formed amino acid interactions compared to the co-crystallized TCU inhibitor (docked, **18**) as represented in (**Tables 4** and **5**). At the same time, germacrene B (**4**), (-)-elema-1,3,11(13)-trien-12-ol (**2**), and isoserinenine (**5**) compounds showed very good binding scores which were very close to that of the docked co-crystallized TCU inhibitor (**18**) with score values of -6.34, -6.30, and -6.25, respectively (**Table 4**).

**Table 4:** Binding scores and interactions of the seventeen isolated and identified compounds from myrrh resin (**1-17**) compared to TCU (docked, **18**) inside the binding pocket of JNK-1.

| No. | Compound  | S <sup>a</sup> | RMSD <sup>b</sup> | Amino acid bond  | Length (Å)   |
|-----|---|----------------|-------------------|--|--|
| 1   | R(+)-Limonene   | -4.96          | 1.51              | -  | -  |
| 2   | (-)-Elema-1,3,11(13)-trien-12-ol                                | <b>-6.30</b>   | <b>0.98</b>       | <b>Met108/H-donor</b>  | <b>3.88</b>  |
| 3   | Curzerene   | -5.76          | 1.12              | Val40/pi-H   | 4.20   |
| 4   | <b>Germacrene B</b>   | <b>-6.34</b>   | <b>0.86</b>       | -  | -  |
| 5   | <b>Isosericenine</b>  | <b>-6.25</b>   | <b>1.28</b>       | <b>Met108/H-donor</b><br><b>Ser155/pi-H</b>  | <b>3.74</b><br><b>3.84</b>   |
| 6   | 3-[(E)-2-phenyl-1-propenyl]cyclohexanone                        | -6.04          | 1.63              | -  | -  |
| 7   | 2,5,8-Trimethyl-1-nonen-3-YN-5-ol                               | -6.00          | 1.43              | Asn114/H-donor<br>Ser155/H-acceptor  | 2.98<br>3.29   |
| 8   | Beta selinene   | -5.65          | 1.38              | -  | -  |
| 9   | Spathulenol   | -5.63          | 1.08              | Ser155/H-donor   | 2.80   |
| 10  | 1-Deoxycapsidiol  | -5.63          | 1.13              | -  | -  |
| 11  | (-)-Caryophyllene oxide   | -5.43          | 0.91              | Asn114/H-acceptor  | 2.87   |
| 12  | <b>Oxalic acid, hexyl 2-methylphenyl ester</b>                  | <b>-7.19</b>   | <b>1.25</b>       | <b>Asn114/H-acceptor</b>   | <b>2.90</b>  |
| 13  | (-)-(R)-Ipsdienol   | -5.30          | 2.08              | Ser155/H-donor<br>Asn114/H-acceptor  | 2.99<br>3.15   |
| 14  | 2-(2-Hydroxy-2-methyl-2-phenylethyl)-3-methyl                   | -6.00          | 1.53              | Val40/pi-H   | 4.15   |
| 15  | Myrcenol  | -5.57          | 1.03              | Ser155/H-donor<br>Asn114/H-acceptor  | 2.96<br>3.32   |
| 16  | 2,8-Decadiene   | -5.26          | 0.55              | -  | -  |
| 17  | Bicyclo[3.1.1]hept-2-ene-2-carboxaldehyde, 6,6-dimethyl-, (1S)- | -4.91          | 1.03              | Gln37/H-acceptor   | 3.24   |
| 18  | <b>Docked co-crystallized inhibitor</b>                         | <b>-6.95</b>   | <b>1.18</b>       | <b>Met111/H-donor</b><br><b>Gln117(H<sub>2</sub>O515)/H-acceptor</b><br><b>Met111/H-acceptor</b><br><b>Gln117(H<sub>2</sub>O515)/H-donor</b><br><b>Glu109/H-donor</b><br><b>Met108/H-donor</b> | <b>2.95</b><br><b>2.99</b><br><b>3.03</b><br><b>3.04</b><br><b>3.19</b><br><b>3.43</b> |

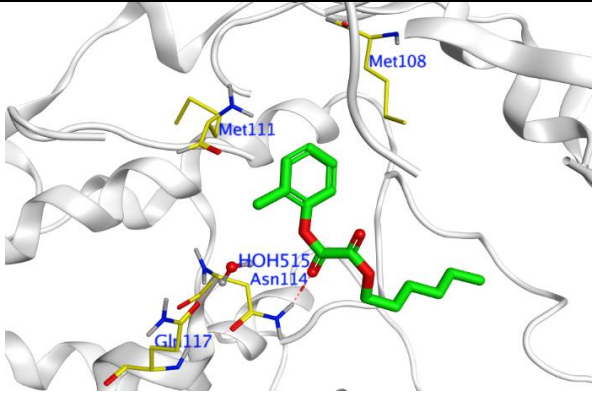
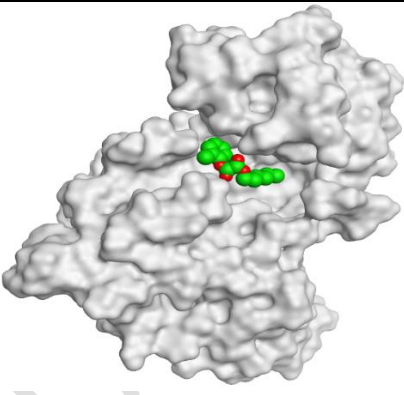
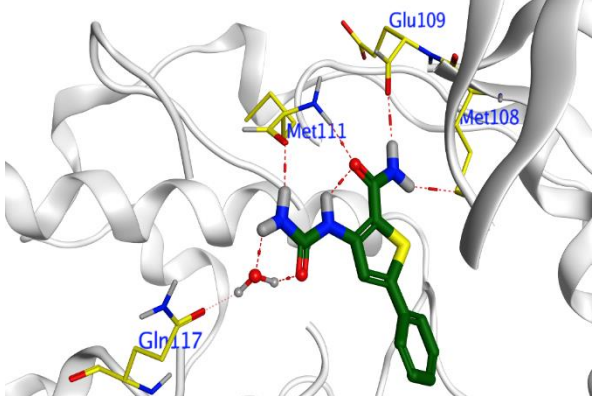
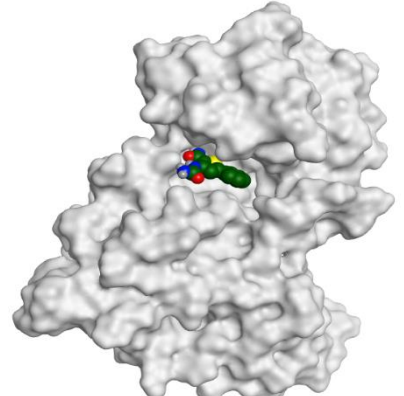
<sup>a</sup> **S**: the score of a compound inside the protein binding pocket (Kcal/mol),

<sup>b</sup> **RMSD**: The Root Mean Squared Deviation between the predicted pose and the crystal structure.



**Table 5:** 3D binding interactions and positioning between the most promising tested compound of myrrh resin (Oxalic acid, hexyl 2-methyl phenyl ester, **12**) at the JNK-binding pocket compared to TCU (docked, **18**).

The red dash represents H-bonds and the black dash represents H-pi interactions.

| Compound | 3 D interactions  | 3 D positioning  |
|----------|---|--|
| 12       |  <p>Diagram showing the 3D interactions of compound <b>12</b> (Oxalic acid, hexyl 2-methyl phenyl ester) within the JNK-binding pocket. The protein backbone is shown as a grey ribbon. Residues Met108, Met111, HOH515, Asn114, and Glu117 are highlighted in yellow. Red dashed lines indicate hydrogen bonds between the compound and these residues. Black dashed lines indicate hydrophobic interactions between the compound and the protein backbone.</p> |  <p>Diagram showing the 3D positioning of compound <b>12</b> within the JNK-binding pocket. The protein surface is shown as a grey mesh, and the compound is shown as a green stick model.</p>  |
| 18       |  <p>Diagram showing the 3D interactions of compound <b>18</b> (TCU) within the JNK-binding pocket. The protein backbone is shown as a grey ribbon. Residues Glu109, Met111, Met108, and Gln117 are highlighted in yellow. Red dashed lines indicate hydrogen bonds between the compound and these residues. Black dashed lines indicate hydrophobic interactions between the compound and the protein backbone.</p>   |  <p>Diagram showing the 3D positioning of compound <b>18</b> within the JNK-binding pocket. The protein surface is shown as a grey mesh, and the compound is shown as a green stick model.</p> |

Regarding the docking results of the isolated tested compounds of myrrh resin compared to TCU, represented a good idea concerning their binding affinities towards JNK-1. Many isolates of the resin showed ideal and promising binding, which indicates high affinities and predicted intrinsic activities as JNK inhibitors as well.

Collectively, this study proposed the promising affinity of myrrh isolates against JNK-1, especially for oxalic acid, hexyl 2-methyl phenyl ester (**12**) which showed a superior binding affinity compared to the docked co-crystallized TCU inhibitor (**18**). Accordingly, we propose such a compound for further in vitro and in vivo studies to gain an effective anti-inflammatory and subsequently an apoptotic therapeutic against nephrotoxicity. Moreover, the previously studied isolates may be examined either alone or in combinations with each other's against nephrotoxicity

#### 4- Discussion

Mirazid's renal protective effect against experimentally generated nephrotoxicity was investigated in this study. Effects on inflammation, antioxidants, and apoptosis were discovered to be responsible for the renal protective effect, which was mainly due to a modulatory effect on JNK1/iNos pathway. For nephrotoxicity induction, a well-standardized experimental model was used.

Although the benefits of Gentamicin in reducing a wide range of bacterial infections, mostly Gram-negative bacteria, have been demonstrated<sup>73</sup>. Gentamicin-induced renal toxicity which is a major clinical challenge to its wide therapeutic application<sup>1, 74, 75</sup> Gentamicin administration raised serum creatinine and urea levels, as well as kidney/body weight, in the current study. In agreement with this result, through drug-induced free radical generation, gentamicin has been linked to the radical formation and oxidant injury in experimental models<sup>76</sup>. Studies showed that serum urea and creatinine elevation is considered to be an important marker of renal dysfunction (glomerular damage marker)<sup>77</sup>. The most sensitive markers for kidney disease detection in experimental trials were serum creatinine, blood urea nitrogen, and kidney weight/body index, which were all raised by gentamicin<sup>77, 78</sup>.

A sensitive indicator of tubular injury is the LDH enzyme found in the proximal renal tubules<sup>79</sup>. LDH activity was considerably higher in the Gentamicin group than in the control group. This increase can be explained by the fact that Gentamicin administration caused a change in redox status, which was demonstrated by a decrease in the concentration of glutathione and an increase in lipid peroxidation<sup>80</sup>.

Inflammation causes a wide spectrum of inflammatory mediators to be released. It is characterized by tissue destruction and secretion of many inflammatory cytokines<sup>81, 82</sup>. When these cells are activated, more cytokines such as nuclear factor kappa B (NF- $\kappa$ B) and iNOS are generated. iNOS causes inflammatory cells to migrate to the wounded area and generates cytokines such as NF- $\kappa$ B<sup>83</sup>. Gentamicin caused peroxynitrite production by inducing the expression of iNOS in glomeruli and mesangial cells<sup>84</sup>. Gentamicin-induced nephrotoxicity is also suggested as a result of nitric oxide(NO) overproduction<sup>85</sup>. Lee *et al.* showed that NO is produced during inflammation<sup>86</sup>. These findings corroborated the results of the current investigation, which indicated Gentamicin's nephrotoxicity.

The decline in antioxidant enzyme activity could be indicative of the negative impacts of Gentamicin. This is in alignment with Abdel-Zaher *et al.*<sup>87</sup> when it comes to Probuocol's effect in

preventing nephrotoxicity triggered by Gentamicin was studied in rats, and also in line with Pai, P.G., *et al.*<sup>88</sup> where the protective action of ursolic acid is activated against Gentamicin nephrotoxicity was studied<sup>88</sup>. The main mechanism by which Gentamicin mediates kidney injury is oxidative stress.

The level of MDA in the Gentamicin group was significantly greater than in the control group, whereas the content of GSH was significantly lower in the Gentamicin group than in the control group. These findings were in line with earlier research which reported that ROS has a significant impact on renal disease pathophysiology<sup>89</sup>. Gentamicin increases ROS production *in vivo* and *in vitro* by modifying mitochondrial respiration. According to Khan *et al.*, free radicals and ROS mediate polyunsaturated fatty acid peroxidation (PUFAs). An overabundance of PUFAs increases the kidneys' vulnerability to ROS<sup>90</sup>. Biological membranes contain significant amounts of PUFAs that are especially vulnerable to lipid peroxide-producing peroxidative attacks<sup>91</sup>.

The Gentamicin group had tubular degradation and necrosis, as well as mononuclear cell infiltration, as demonstrated in the histological image of the kidney tissues. The discovered histopathological renal changes as a result of nephrotoxicity induced by Gentamicin are consistent with findings from Kuatsienu *et al.*<sup>92</sup> Alarifi *et al.* reported, necrosis, degeneration, and vacuolization were early signs of tubular changes caused by gentamicin treatment. By the conclusion of the gentamicin treatment, tubular abnormalities in the kidney had emerged, and their severity had grown. The majority of the proximal convoluted tubules and, to a lesser extent, the distal tubules were affected by degeneration up to severe necrosis<sup>93</sup>.

The activation of the apoptotic pathway was linked to Gentamicin-induced kidney damage, implying that the apoptotic pathway was linked to renal damage caused by Gentamicin. According to the study, NF- $\kappa$ B activation enhanced Gentamicin-induced apoptosis in rat tubular cells<sup>94</sup>. The considerable increases in caspase3 expression in renal cortical tissue revealed that Gentamicin produced endoplasmic reticulum (ER) stress and activation of ER-mediated cell death indicators in this investigation<sup>95</sup>. One of the fundamental processes that provide protection and repair in stress-induced cellular dysfunction by inducing cell death is the activation of ER stress<sup>96</sup>.

In the current study, Mirazid prophylactic showed a reno-protective effect against Gentamicin triggered nephrotoxicity, Gentamicin-induced nephrotoxicity was significantly improved, as seen by considerable reductions in (creatinine, urea, and LDH) levels and kidney weight. These findings support Hanan's findings that Mirazid therapy improved renal function in rats<sup>97</sup>. Numerous experimental animal models have shown a relationship between oxidative stress and

nephrotoxicity<sup>50</sup>. Furthermore, it has been demonstrated that treating rats with hydroxyl radical scavengers protects them against acute renal failure caused by Gentamicin<sup>98</sup>.

Prophylactic treatment with Mirazid showed inhibition of kidney oxidative stress. It reduced MDA levels, meaning that it inhibited lipid peroxidation and the production of ROS, which was accompanied by increased GSH content, implying a significant boost in antioxidant defenses. Significant reductions in serum LDH activity accompanied these improvements in oxidative/antioxidant balance. Mirazid's capacity to prevent lipid peroxidation and dramatically improve the activity of antioxidant enzymes has been established in previous research to have a protective impact<sup>23</sup>. Various studies have reported findings that are consistent with the ones presented here, Polyphenolic groups in myrrh extract induce a protective action against ROS<sup>99, 100</sup>. Due to its free radical-scavenging properties, it exhibited a preventive effect against stomach ulcers<sup>101</sup>. It was recently discovered that myrrh, a powerful antioxidant, works by enhancing the total antioxidant activity of the serum and tissues.<sup>99</sup> Meanwhile, Mirazid inhibited the production of MDA in Gentamicin induced renal cells<sup>102</sup>. Improved antioxidant defense and reduced ROS generation can help maintain cellular integrity and provide structural, biochemical, and physiological benefits<sup>103</sup>. Mirazid's antioxidant properties were associated with a significant decrease in Pathological alterations caused by gentamicin, as well as a return to normal metabolic equilibrium and cellular hemostasis<sup>104</sup>. Mirazid has been proven to protect the nephrons, which is assumed to be related to its antioxidant effects<sup>99</sup> and the antioxidants attenuate lipid peroxidation induced by Gentamicin<sup>105</sup>.

In this study, there was an elevation in the expression of iNOS and JNK1. This can be explained by; Gentamicin administration has led to stimulation of inflammatory pathways through the upregulation of iNOS expressions. Furthermore, tumor necrosis factor-alpha (TNF- $\alpha$ ) is a pro-inflammatory cytokine produced by glomerular and tubular cells, as well as extrinsic inflammatory cells, in response to Gentamicin treatment. TNF- $\alpha$  operates through the mitogen-activated protein kinase (MAPK) and NF- $\kappa$ B signaling pathways<sup>106</sup>. Tissue damage and inflammation are important nephrotoxicity triggers<sup>107</sup>. Furthermore, Gentamicin activates the signaling pathways of MAPK<sup>108</sup>. JNK1 is one of three well-known MAPK pathways; it is regarded as a pro-inflammatory pathway. Cell proliferation, differentiation, migration, and apoptosis are also controlled<sup>109</sup>. The effect of Gentamicin obtained in the current study can be explained by these findings (**Figure 6**).

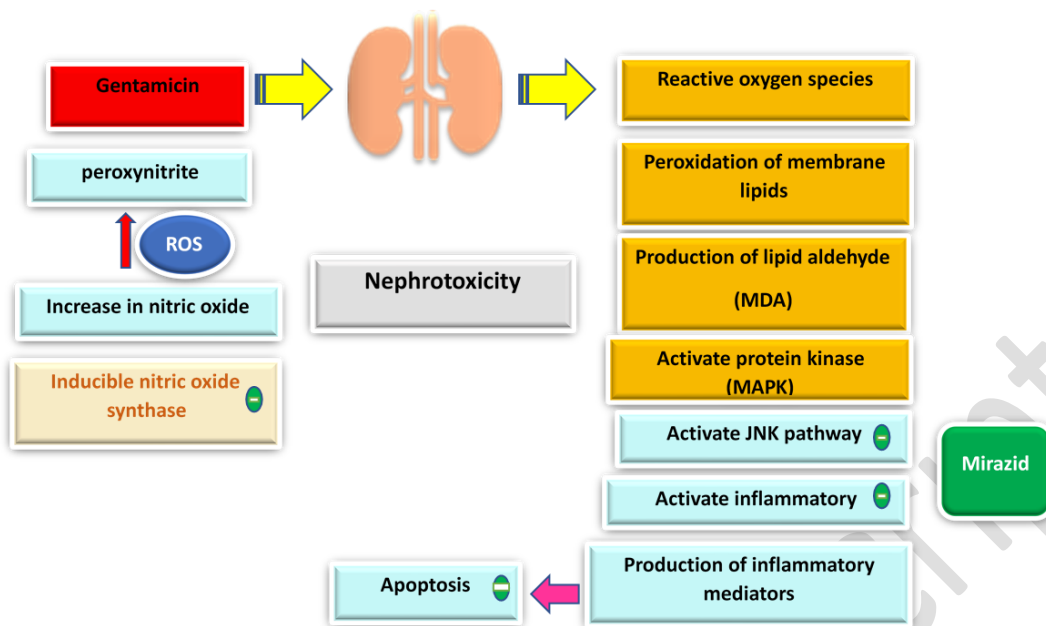


**Figure (6):** The protective role of Mirazid in Gentamicin-induced nephrotoxicity.

Gentamicin caused nephrotoxicity by increasing membrane lipid peroxidation and the formation of lipid aldehyde by stimulating ROS. JNK1 is one of three well-known MAPK pathways that activate protein kinase.; it is regarded as a pro-apoptotic and pro-inflammatory pathway<sup>110</sup>. JNK activates the apoptosis pathway and the production of inflammatory markers. Gentamicin induced inducible nitric oxide synthase expression in glomeruli and mesangial cells and caused peroxynitrite production. This results in insult of inflammation and damage of the glomerulus (Nephrotoxicity). Mirazid possesses nephroprotective benefits due to its antioxidant, anti-inflammatory, and anti-apoptotic qualities.

Mirazid's anti-inflammatory and immune-modulating properties are confirmed by a reduction in renal iNOS content. In agreement with these results, the transcription factor NF- $\kappa$ B and MAPK that regulate the expression of many immune and inflammatory genes were inhibited by Mirazid, and several inflammatory mediators needed for initiation, maintenance of an inflammatory process, and reduction of oxidative stress were modulated by Mirazid<sup>50</sup>. Because it regulates genes and coordinates the expression of pro-inflammatory enzymes and cytokines including iNOS and TNF- $\alpha$ , as well as interleukin-6, NF- $\kappa$ B is generally understood to be critical for cell viability (IL-6)<sup>111</sup>. In inflammatory and immune reactions, the NO radical is recognized to have a central role<sup>112, 113</sup>. iNOS is inactive in resting cells under normal physiological conditions, but it produces a large amount of NO under pathological conditions, resulting in interferon (IFN) and lipopolysaccharide (LPS)

increased endothelial nitric oxide synthase (eNOS) levels 10 times, which has a dual function in chronic infection, inflammation, and carcinogenesis<sup>114</sup>.

Mitigation of Gentamicin-induced histological alterations confirm the anti-inflammatory impact of mirazid; of worth, choosing is the significant downregulation of apoptotic and inflammatory responses. Mirazid caused caspase-3 expression to decrease, indicating that apoptosis was retracted<sup>94</sup>. In light of the situation, by inhibiting the activation of the ER stress and NF- $\kappa$ B pathways, Mirazid protected cells from apoptosis. These mechanisms that have been proposed are backed up by prior research that found Mirazid is an effective free radical scavenger in the kidney inhibiting inflammatory signaling pathways and preventing gentamicin-induced renal toxicity<sup>50</sup>.

## 5- Conclusion

Finally, by blocking the JNK1/iNOS pathway, Mirazid generates anti-inflammatory, anti-oxidant, and anti-apoptotic effects, as demonstrated in this study. Molecular docking was used to investigate seventeen identified chemicals from myrrh resin using GC-MS and ICP-MS separation techniques against JNK-1 which is responsible for stopping both the apoptotic and iNOS pathways and therefore proposed to be the main mechanism of action for its anti-inflammatory effects. Among the tested isolates oxalic acid, hexyl 2-methyl phenyl ester (**12**) was found to be superior to the docked co-crystallized inhibitor (**18**) with a binding score of -7.19 kcal/mol compared to -6.95, respectively. Our findings could help in the exact identification of the main constituents of myrrh responsible for its anti-inflammatory effects by targeting JNK-1. Especially oxalic acid, hexyl 2-methyl phenyl ester (**12**), germacrene B (**4**), (-)-elema-1,3,11(13)-trien-12-ol (**2**), and isosericenine (**5**) isolates represent the most promising compounds for further preclinical and clinical studies for the treatment of inflammation.

## **Author Contributions**

Conceptualization: SAA, AEK; Data curation: AAA, MM, MAE, and AEK; Formal Analysis: AAA, MM, MAE, SS, and AEK; Methodology: AAA, AM, MM, MAE, SS, and AEK; Project administration: AAA and AEK; Resources: AAA and AEK; Supervision: AAA and AEK; Validation: SAA, AAA, and AEK; Visualization: AAA, AM, SS, and AEK; Writing – original draft: SAA, AAA, AM, SS, and AEK; Writing– review and editing: SAA, AAA, and AEK. All authors approved the final version of the manuscript.

## **Conflict of interest**

The authors declare no conflict of interest.

## **Acknowledgment**

The authors thank Dr. Walaa Fekrey, professor of Pathology at Mansoura University's Faculty of Veterinary Medicine in Egypt, for her assistance in conducting histopathological and immunohistochemical analyses.

## References

1. Mingeot-Leclercq, M.-P.; Tulkens, P. M. Aminoglycosides: nephrotoxicity. *Antimicrob Agents Chemother.* 1999, 43, 1003-1012. DOI: <https://doi.org/10.1128/AAC.43.5.1003>
2. Ayla, S.; Seckin, I.; Tanriverdi, G.; Cengiz, M.; Eser, M.; Soner, B.; Oktem, G. Doxorubicin induced nephrotoxicity: protective effect of nicotinamide. *Int J Biochem Cell Biol.* 2011. DOI: <https://doi.org/10.1155/2011/390238>
3. Karaman, A.; Fadillioglu, E.; Turkmen, E.; Tas, E.; Yilmaz, Z. Protective effects of leflunomide against ischemia-reperfusion injury of the rat liver. *Pediatr Surg Int.* 2006, 22, 428-434. DOI: [10.1007/s00383-006-1668-x](https://doi.org/10.1007/s00383-006-1668-x)
4. Kang, C.; Lee, H.; Hah, D.-Y.; Heo, J. H.; Kim, C. H.; Kim, E.; Kim, J. S. Protective effects of *Houttuynia cordata* Thunb. on gentamicin-induced oxidative stress and nephrotoxicity in rats. *Toxicol Res.* 2013, 29, 61-67. DOI: <https://doi.org/10.5487/TR.2013.29.1.061>
5. Lopez-Novoa, J. M.; Quiros, Y.; Vicente, L.; Morales, A. I.; Lopez-Hernandez, F. J. New insights into the mechanism of aminoglycoside nephrotoxicity: an integrative point of view. *Kidney int.* 2011, 79, 33-45. DOI: <https://doi.org/10.1038/ki.2010.337>
6. Heart, E. A.; Karandrea, S.; Liang, X.; Balke, M. E.; Beringer, P. A.; Bobczynski, E. M.; Zayas-Bazán Burgos, D.; Richardson, T.; Gray, J. P. Mechanisms of Doxorubicin Toxicity in Pancreatic  $\beta$ -Cells. *Toxicol Sci.* 2016, 152, 395-405. DOI: <https://doi.org/10.1093/toxsci/kfw096>
7. Balakumar, P.; Rohilla, A.; Thangathirupathi, A. Gentamicin-induced nephrotoxicity: do we have a promising therapeutic approach to blunt it? *Pharmacol Res.* 2010, 62, 179-186. DOI: <https://doi.org/10.1016/j.phrs.2010.04.004>
8. Helal, M. G.; Zaki, M. M. A. F.; Said, E. J. Nephroprotective effect of saxagliptin against gentamicin-induced nephrotoxicity, emphasis on anti-oxidant, anti-inflammatory and anti-apoptic effects. *Life sciences.* 2018, 208, 64-71. DOI: <https://doi.org/10.1016/j.lfs.2018.07.021>
9. Cao, L.; Zhi, D.; Han, J.; Kumar Sah, S.; Xie, Y. Combinational effect of curcumin and metformin against gentamicin-induced nephrotoxicity: Involvement of antioxidative, anti-inflammatory and antiapoptotic pathway. *J Food Biochem.* 2019, 43, e12836. DOI: <https://doi.org/10.1111/jfbc.12836>
10. Shahani, S.; Behzadfar, F.; Jahani, D.; Ghasemi, M.; Shaki, F. Antioxidant and anti-inflammatory effects of *Nasturtium officinale* involved in attenuation of gentamicin-induced nephrotoxicity. *Toxicol Mech Methods.* 2017, 27, 107-114. DOI: <https://doi.org/10.1080/15376516.2016.1258748>
11. Kontush, A.; Chapman, M. J. Functionally defective high-density lipoprotein: a new therapeutic target at the crossroads of dyslipidemia, inflammation, and atherosclerosis. *Pharmacol Rev.* 2006, 58, 342-374. DOI: <https://doi.org/10.1124/pr.58.3.1>
12. Hansson, G. K.; Robertson, A.-K. L.; Söderberg-Nauclér, C. Inflammation and atherosclerosis. *Annu Rev Pathol.* 2006, 1, 297-329. DOI: <https://doi.org/10.1146/annurev.pathol.1.110304.100100>



13. Kumar, A. P.; Ryan, C.; Cordy, V.; Reynolds, W. Inducible nitric oxide synthase expression is inhibited by myeloperoxidase. *Nitric oxide*. 2005, 13, 42-53. DOI: <https://doi.org/10.1016/j.niox.2005.04.002>
14. Greene, D. Gold, frankincense, myrrh, and medicine. *N C Med J*. 1993, 54, 620-622. PMID: [8302372](https://pubmed.ncbi.nlm.nih.gov/8302372/)
15. Badria, F.; Abou-Mohamed, G.; El-Mowafy, A.; Masoud, A.; Salama, O. Mirazid: a new schistosomicidal drug. *Pharm Biol*. 2001, 39, 127-131. DOI: <https://doi.org/10.1076/phbi.39.2.127.6253>
16. Sheir, Z.; Nasr, A. A.; Massoud, A.; Salama, O.; Badra, G. A.; El-Shennawy, H.; Hassan, N.; Hammad, S. M. A safe, effective, herbal antischistosomal therapy derived from myrrh. *Am. J. Trop. Med. Hyg*. 2001, 65, 700-704.
17. Habtemariam, S. Cytotoxic and cytostatic activity of erlangerins from *Commiphora erlangeriana*. *Toxicon*. 2003, 41, 723-727. DOI: [https://doi.org/10.1016/S0041-0101\(03\)00048-5](https://doi.org/10.1016/S0041-0101(03)00048-5)
18. Shoemaker, M.; Hamilton, B.; Dairkee, S. H.; Cohen, I.; Campbell, M. In vitro anticancer activity of twelve Chinese medicinal herbs. *Phytother Res*. 2005, 19, 649-651. DOI: <https://doi.org/10.1002/ptr.1702>
19. Dolara, P.; Luceri, C.; Ghelardini, C.; Monserrat, C.; Aiolfi, S.; Luceri, F.; Lodovici, M.; Menichetti, S.; Romanelli, M. Analgesic effects of myrrh. *Nature*. 1996, 379, 29-29. DOI: <https://doi.org/10.1038/379029a0>
20. Qureshi, S.; Al-Harbi, M.; Ahmed, M.; Raza, M.; Giangreco, A.; Shah, A. Evaluation of the genotoxic, cytotoxic, and antitumor properties of *Commiphora molmol* using normal and Ehrlich ascites carcinoma cell-bearing Swiss albino mice. *Cancer Chemother Pharmacol*. 1993, 33, 130-138.
21. Chander, R.; Khanna, A.; Kapoor, N. Lipid lowering activity of guggulsterone from *Commiphora mukul* in hyperlipaemic rats. *Phytother Res*. 1996, 10, 508-511. DOI: [https://doi.org/10.1002/\(SICI\)1099-1573\(199609\)10:6<508::AID-PTR895>3.0.CO;2-P](https://doi.org/10.1002/(SICI)1099-1573(199609)10:6<508::AID-PTR895>3.0.CO;2-P)
22. Saeed, M. A.; Sabir, A. J. Antibacterial activities of some constituents from oleo-gum-resin of *Commiphora mukul*. *Fitoterapia*. 2004, 75, 204-208. DOI: [10.1016/j.fitote.2003.12.003](https://doi.org/10.1016/j.fitote.2003.12.003)
23. Kim, M.-S.; Bae, G.-S.; Park, K.-C.; Koo, B. S.; Kim, B.-J.; Lee, H.-J.; Seo, S.-W.; Shin, Y. K.; Jung, W.-S.; Cho, J.-H. Myrrh inhibits LPS-induced inflammatory response and protects from cecal ligation and puncture-induced sepsis. *Evid Based Complement Alternat Med*. 2012, 2012. DOI: <https://doi.org/10.1155/2012/278718>
24. Ghanem, A.; Emara, H. A.; Muawia, S.; Abd El Maksoud, A. I.; Al-Karmalawy, A. A.; Elshal, M. F. Tanshinone IIA synergistically enhances the antitumor activity of doxorubicin by interfering with the PI3K/AKT/mTOR pathway and inhibition of topoisomerase II: in vitro and molecular docking studies. *New J. Chem*. 2020, 44, 17374-17381. DOI: <https://doi.org/10.1039/D0NJ04088F>
25. Soltane, R.; Chrouda, A.; Mostafa, A.; Al-Karmalawy, A. A.; Chouaïb, K.; dhahri, A.; Pashameah, R. A.; Alasiri, A.; Kutkat, O.; Shehata, M.; Jannet, H. B.; Gharbi, J.; Ali, M. Strong Inhibitory Activity and Action Modes of Synthetic Maslinic Acid Derivative on Highly Pathogenic

Coronaviruses: COVID-19 Drug Candidate. *Pathogens*. 2021, 10, 623. DOI: <https://doi.org/10.3390/pathogens10050623>

26. Taher, R. F.; Al-Karmalawy, A. A.; Abd El Maksoud, A. I.; Khalil, H.; Hassan, A.; El-Khrisy, E.-D. A.; El-Kashak, W. Two new flavonoids and anticancer activity of *Hymenospodium flavum*: in vitro and molecular docking studies. *J Herbmed Pharmacol*. 2021, 10, 443-458. DOI: [10.34172/jhp.2021.52](https://doi.org/10.34172/jhp.2021.52)

27. Zaki, A. A.; Ashour, A.; Elhady, S. S.; Darwish, K. M.; Al-Karmalawy, A. A. Calendulaglycoside A Showing Potential Activity Against SARS-CoV-2 Main Protease: Molecular Docking, Molecular Dynamics, and SAR Studies. *J Tradit Complement Med*. 2021. DOI: <https://doi.org/10.1016/j.jtcme.2021.05.001>

28. Zaki, A. A.; Al-Karmalawy, A. A.; Khodir, A. E.; El-Amier, Y. A.; Ashour, A. Isolation of cytotoxic active compounds from *Reichardia tingitana* with investigation of apoptosis mechanistic induction: In silico, in vitro, and SAR studies. *S Afr J Bot*. 2022, 144, 115-123. DOI: <https://doi.org/10.1016/j.sajb.2021.08.006>

29. Shoala, T.; Al-Karmalawy, A. A.; Germoush, M. O.; Al-Shamrani, S. M.; Abdein, M. A.; Awad, N. S. Nanobiotechnological Approaches to Enhance Potato Resistance against Potato Leafroll Virus (PLRV) Using Glycyrrhizic Acid Ammonium Salt and Salicylic Acid Nanoparticles. *Horticulturae*. 2021, 7, 402. DOI: <https://doi.org/10.3390/horticulturae7100402>

30. Raslan, M. A.; F. Taher, R.; Al-Karmalawy, A. A.; El-Ebeedy, D.; Metwaly, A. G.; Elkateeb, N. M.; Ghanem, A.; Elghaish, R. A.; Abd El Maksoud, A. I. *Cordyline fruticosa* (L.) A. Chev. leaves: isolation, HPLC/MS profiling and evaluation of nephroprotective and hepatoprotective activities supported by molecular docking. *New J. Chem*. 2021. DOI: <https://doi.org/10.1039/D1NJ02663A>

31. Brogi, S. Computational approaches for drug discovery. *Molecules*. 2019. DOI: <https://doi.org/10.3390/molecules24173061>

32. Elmaaty, A. A.; Alnajjar, R.; Hamed, M. I.; Khattab, M.; Khalifa, M. M.; Al-Karmalawy, A. A. Revisiting activity of some glucocorticoids as a potential inhibitor of SARS-CoV-2 main protease: theoretical study. *RSC Adv*. 2021, 11, 10027-10042. DOI: [10.1039/D0RA10674G](https://doi.org/10.1039/D0RA10674G)

33. Mahmoud, D. B.; Ismail, W. M.; Moatasim, Y.; Kutkat, O.; ElMeshad, A. N.; Ezzat, S. M.; El Deeb, K. S.; El-Fishawy, A. M.; Gomaa, M. R.; Kandeil, A.; Al-karmalawy, A. A.; Ali, M. A.; Mostafa, A. Delineating a potent antiviral activity of *Cuphea ignea* extract loaded nano-formulation against SARS-CoV-2: In silico and in vitro studies. *J Drug Deliv Sci Technol*. 2021, 102845. DOI: <https://doi.org/10.1016/j.jddst.2021.102845>

34. Khalifa, M. M.; Al-Karmalawy, A. A.; Elkaeed, E. B.; Nafie, M. S.; Tantawy, M. A.; Eissa, I. H.; Mahdy, H. A. Topo II inhibition and DNA intercalation by new phthalazine-based derivatives as potent anticancer agents: design, synthesis, anti-proliferative, docking, and in vivo studies. *J Enzyme Inhib Med Chem*. 2022, 37, 299-314. DOI: <https://doi.org/10.1080/14756366.2021.2007905>

35. Mahmoud, A.; Mostafa, A.; Al-Karmalawy, A. A.; Zidan, A.; Abulkhair, H. S.; Mahmoud, S. H.; Shehata, M.; Elhefnawi, M. M.; Ali, M. A. Telaprevir is a potential drug for repurposing against SARS-CoV-2: computational and in vitro studies. *Heliyon*. 2021, 7. DOI: <https://doi.org/10.1016/j.heliyon.2021.e07962>

36. Mahmoud, A.; Kotb, E.; Alqosaibi, A. I.; Al-Karmalawy, A. A.; Al-Dhuayan, I. S.; Alabkari, H. In vitro and in silico characterization of alkaline serine protease from *Bacillus subtilis* D9 recovered from Saudi Arabia. *Heliyon*. 2021, 7, e08148. DOI: <https://doi.org/10.1016/j.heliyon.2021.e08148>
37. Khattab, M.; Al-Karmalawy, A. A. Computational repurposing of benzimidazole anthelmintic drugs as potential colchicine binding site inhibitors. *Future Med Chem*. 2021, 13, 19. DOI: <https://doi.org/10.4155/fmc-2020-0273>
38. Kandeil, A.; Mostafa, A.; Kutkat, O.; Moatasim, Y.; Al-Karmalawy, A. A.; Rashad, A. A.; Kayed, A. E.; Kayed, A. E.; El-Shesheny, R.; Kayali, G.; Ali, M. A. Bioactive Polyphenolic Compounds Showing Strong Antiviral Activities against Severe Acute Respiratory Syndrome Coronavirus 2. *Pathogens*. 2021, 10, 758. DOI: <https://doi.org/10.3390/pathogens10060758>
39. Elshal, M. F. Concanavalin-A shows synergistic cytotoxicity with tamoxifen via inducing apoptosis in estrogen receptor-positive breast cancer. *Pharm Sci*. 2021. DOI: [10.34172/PS.2021.22](https://doi.org/10.34172/PS.2021.22)
40. Gaber, A. A.; El-Morsy, A. M.; Sherbiny, F. F.; Bayoumi, A. H.; El-Gamal, K. M.; El-Adl, K.; Al-Karmalawy, A. A.; Ezz Eldin, R. R.; Saleh, M. A.; Abulkhair, H. S. Pharmacophore-linked pyrazolo[3,4-d]pyrimidines as EGFR-TK inhibitors: Synthesis, anticancer evaluation, pharmacokinetics, and in silico mechanistic studies. *Arch Pharm*. 2021, e2100258. DOI: <https://doi.org/10.1002/ardp.202100258>
41. El-Shershaby, M. H.; Ghiaty, A.; Bayoumi, A. H.; Al-Karmalawy, A. A.; Hussein, E. M.; El-Zoghbi, M. S.; Abulkhair, H. S. From triazolophthalazines to triazoloquinazolines: A biososterism-guided approach toward the identification of novel PCAF inhibitors with potential anticancer activity. *Bioorg Med Chem*. 2021, 42, 116266. DOI: <https://doi.org/10.1016/j.bmc.2021.116266>
42. El-Shershaby, M. H.; El-Gamal, K. M.; Bayoumi, A. H.; El-Adl, K.; Alswah, M.; Ahmed, H. E. A.; Al-Karmalawy, A. A.; Abulkhair, H. S. The antimicrobial potential and pharmacokinetic profiles of novel quinoline-based scaffolds: synthesis and in silico mechanistic studies as dual DNA gyrase and DHFR inhibitors. *New J. Chem*. 2021. DOI: [10.1039/D1NJ02838C](https://doi.org/10.1039/D1NJ02838C)
43. Elebeedy, D.; Elkhatib, W. F.; Kandeil, A.; Ghanem, A.; Kutkat, O.; Alnajjar, R.; Saleh, M. A.; Abd El Maksoud, A. I.; Badawy, I.; Al-Karmalawy, A. A. Anti-SARS-CoV-2 activities of tanshinone IIA, carnosic acid, rosmarinic acid, salvianolic acid, baicalein, and glycyrrhetic acid between computational and in vitro insights. *RSC Adv*. 2021, 11, 29267-29286. DOI: [10.1039/D1RA05268C](https://doi.org/10.1039/D1RA05268C)
44. Elebeedy, D.; Badawy, I.; Elmaaty, A. A.; Saleh, M. M.; Kandeil, A.; Ghanem, A.; Kutkat, O.; Alnajjar, R.; Abd El Maksoud, A. I.; Al-karmalawy, A. A. In vitro and computational insights revealing the potential inhibitory effect of Tanshinone IIA against influenza A virus. *Comput Biol Med*. 2021, 105149. DOI: <https://doi.org/10.1016/j.compbiomed.2021.105149>
45. Hazem, R. M.; Antar, S. A.; Nafea, Y. K.; Al-Karmalawy, A. A.; Saleh, M. A.; El-Azab, M. F. Pirfenidone and vitamin D mitigate renal fibrosis induced by doxorubicin in mice with Ehrlich solid tumor. *Life Sciences*. 2021, 120185. DOI: <https://doi.org/10.1016/j.lfs.2021.120185>
46. Hamed, M. I. A.; Darwish, K. M.; Soltane, R.; Chrouda, A.; Mostafa, A.; Abo Shama, N. M.; Elhady, S. S.; Abulkhair, H. S.; Khodir, A. E.; Elmaaty, A. A.; Al-karmalawy, A. A.  $\beta$ -Blockers

bearing hydroxyethylamine and hydroxyethylene as potential SARS-CoV-2 Mpro inhibitors: rational based design, in silico, in vitro, and SAR studies for lead optimization. RSC Adv. 2021, 11, 35536-35558. DOI: [10.1039/D1RA04820A](https://doi.org/10.1039/D1RA04820A)

47. Elmaaty, A. A.; Darwish, K. M.; Khattab, M.; Elhady, S. S.; Salah, M.; Hamed, M. I. A.; Al-Karmalawy, A. A.; Saleh, M. M. In a search for potential drug candidates for combating COVID-19: computational study revealed salvianolic acid B as a potential therapeutic targeting 3CL<sub>pro</sub> and spike proteins. J Biomol Struct Dyn. 2021, 1-28. DOI: <https://doi.org/10.1080/07391102.2021.1918256>

48. Elmaaty, A. A.; Darwish, K. M.; Chrouda, A.; Boseila, A. A.; Tantawy, M. A.; Elhady, S. S.; Shaik, A. B.; Mustafa, M.; Al-karmalawy, A. A. In Silico and In Vitro Studies for Benzimidazole Anthelmintics Repurposing as VEGFR-2 Antagonists: Novel Mebendazole-Loaded Mixed Micelles with Enhanced Dissolution and Anticancer Activity. ACS Omega. 2021. DOI: <https://doi.org/10.1021/acsomega.1c05519>

49. Elia, S. G.; Al-Karmalawy, A. A.; Nasr, M. Y.; Elshal, M. F. Loperamide potentiates doxorubicin sensitivity in triple-negative breast cancer cells by targeting MDR1 and JNK and suppressing mTOR and Bcl-2: In vitro and molecular docking study. J Biochem Mol Toxicol. 2021, 36, 1, e22938. DOI: <https://doi.org/10.1002/jbt.22938>

50. AbdEl-Mongy, M.; Nasr, M. Y.; Elsayed, I. H.; Soliman, A. M. J. J. o. B. Antioxidant and histopathological effects of mirazid on gentamicin-induced renal damage in rats. J Biochem Microbiol Biotechnol. 2015, 3, 10-14. DOI: <https://doi.org/10.54987/jobimb.v3i1.229>

51. Kaplan, A. A.; Kohn, O. F. Fractional excretion of urea as a guide to renal dysfunction. Am J Nephrol. 1992, 12, 49-54. DOI: <https://doi.org/10.1159/000168417>

52. Ohkawa, H.; Ohishi, N.; Yagi, K. Reaction of linoleic acid hydroperoxide with thiobarbituric acid. J Lipid Res. 1978, 19, 1053-1057. DOI: [https://doi.org/10.1016/S0022-2275\(20\)40690-X](https://doi.org/10.1016/S0022-2275(20)40690-X)

53. Ellman, G. L. Tissue sulfhydryl groups. Arch Biochem Biophys. 1959, 82, 70-77.

54. Ahamad, S. R.; Al-Ghadeer, A. R.; Ali, R.; Qamar, W.; Aljarboa, S. Analysis of inorganic and organic constituents of myrrh resin by GC-MS and ICP-MS: An emphasis on medicinal assets. Saudi Pharm J. 2017, 25, 788-794. DOI: <https://doi.org/10.1016/j.jsps.2016.10.011>

55. El-Demerdash, A.; Al-Karmalawy, A. A.; Abdel-Aziz, T. M.; Elhady, S. S.; Darwish, K. M.; Hassan, A. H. E. Investigating the structure-activity relationship of marine natural polyketides as promising SARS-CoV-2 main protease inhibitors. RSC Adv. 2021, 11, 31339-31363. DOI: [10.1039/D1RA05817G](https://doi.org/10.1039/D1RA05817G)

56. El Gizawy, H. A.; Boshra, S. A.; Mostafa, A.; Mahmoud, S. H.; Ismail, M. I.; Alsouk, A. A.; Taher, A. T.; Al-Karmalawy, A. A. Pimenta dioica (L.) Merr. Bioactive Constituents Exert Anti-SARS-CoV-2 and Anti-Inflammatory Activities: Molecular Docking and Dynamics, In Vitro, and In Vivo Studies. Molecules. 2021, 26, 5844. DOI: <https://doi.org/10.3390/molecules26195844>

57. Samra, R. M.; Soliman, A. F.; Zaki, A. A.; Ashour, A.; Al-Karmalawy, A. A.; Hassan, M. A.; Zaghoul, A. M. Bioassay-guided isolation of a new cytotoxic ceramide from *Cyperus rotundus* L. S Afr J Bot. 2021, 139, 210-216. DOI: <https://doi.org/10.1016/j.sajb.2021.02.007>

58. Khattab, M.; Al- Karmalawy, A. A. Revisiting Activity of Some Nocodazole Analogues as a Potential Anticancer Drugs Using Molecular Docking and DFT Calculations. *Front Chem.* 2021, 9, 92. DOI: [10.3389/fchem.2021.628398](https://doi.org/10.3389/fchem.2021.628398)
59. Diab, R. T.; Abdelsamii, Z.; Abd-Elaal, E. H.; Al-Karmalawy, A. A.; AboDya, N. E. Design and Synthesis of a New Series of 3,5-Disubstituted-1,2,4-Oxadiazoles as Potential Colchicine Binding Site Inhibitors: Antiproliferative activity, Molecular docking, and SAR Studies. *New J Chem.* 2021. DOI: [10.1039/D1NJ02885E](https://doi.org/10.1039/D1NJ02885E)
60. Oza, V.; Ashwell, S.; Almeida, L.; Brassil, P.; Breed, J.; Deng, C.; Gero, T.; Grondine, M.; Horn, C.; Ioannidis, S. Discovery of checkpoint kinase inhibitor (S)-5-(3-fluorophenyl)-N-(piperidin-3-yl)-3-ureidothiophene-2-carboxamide (AZD7762) by structure-based design and optimization of thiophenecarboxamide ureas. *J Med Chem.* 2012, 55, 5130-5142. DOI: <https://doi.org/10.1021/jm300025r>
61. Zaki, A. A.; Al-Karmalawy, A. A.; El-Amier, Y. A.; Ashour, A. J. N. J. o. C. Molecular docking reveals the potential of Cleome amblyocarpa isolated compounds to inhibit COVID-19 virus main protease. *New J Chem.* 2020, 44, 16752-16758. DOI: [10.1039/D0NJ03611K](https://doi.org/10.1039/D0NJ03611K)
62. Al- Karmalawy, A. A.; Eissa, I. H. J. P. S. Molecular docking and dynamics simulations reveal the potential of anti-HCV drugs to inhibit COVID-19 main protease. *Pharm Sci.* 2021. DOI: : [10.34172/PS.2021.3](https://doi.org/10.34172/PS.2021.3)
63. Aziz, M. A.; Shehab, W. S.; Al-Karmalawy, A. A.; EL-Farargy, A. F.; Abdellatif, M. H. Design, Synthesis, Biological Evaluation, 2D-QSAR Modeling, and Molecular Docking Studies of Novel 1H-3-Indolyl Derivatives as Significant Antioxidants. *Int J Mol Sci.* 2021, 22, 10396. DOI: <https://doi.org/10.3390/ijms221910396>
64. Al-Karmalawy, A. A.; Farid, M. M.; Mostafa, A.; Ragheb, A. Y.; H. Mahmoud, S.; Shehata, M.; Shama, N. M. A.; GabAllah, M.; Mostafa-Hedeab, G.; Marzouk, M. M. Naturally Available Flavonoid Aglycones as Potential Antiviral Drug Candidates against SARS-CoV-2. *Molecules.* 2021, 26, 6559. DOI: <https://doi.org/10.3390/molecules26216559>
65. Al-Karmalawy, A. A.; Khattab, M. J. N. J. o. C. Molecular modelling of mebendazole polymorphs as a potential colchicine binding site inhibitor. *New J Chem.* 2020, 44, 13990-13996. DOI: [10.1039/D0NJ02844D](https://doi.org/10.1039/D0NJ02844D)
66. Alnajjar, R.; Mostafa, A.; Kandeil, A.; Al-Karmalawy, A. A. J. H. Molecular docking, molecular dynamics, and in vitro studies reveal the potential of angiotensin II receptor blockers to inhibit the COVID-19 main protease. *Heliyon.* 2020, 6, e05641. DOI: <https://doi.org/10.1016/j.heliyon.2020.e05641>
67. Al-Karmalawy, A. A.; Dahab, M. A.; Metwaly, A. M.; Elhady, S. S.; Elkaeed, E. B.; Eissa, I. H.; Darwish, K. M. Molecular Docking and Dynamics Simulation Revealed the Potential Inhibitory Activity of ACEIs Against SARS-CoV-2 Targeting the hACE2 Receptor. *Front Chem.* 2021, 9. DOI: <https://doi.org/10.3389/fchem.2021.661230>
68. Al-Karmalawy, A.; Ma, C.; Taghour, M. S.; Belal, A.; Mehany, A.; Mostafa, N.; Nabeeh, A.; Eissa, I. Design and Synthesis of New Quinoxaline Derivatives as Potential Histone Deacetylase Inhibitors Targeting Hepatocellular Carcinoma: In Silico, In Vitro, and SAR Studies. *Front Chem.* 2021, 9, 648. DOI: <https://doi.org/10.3389/fchem.2021.725135>

69. McConkey, B. J.; Sobolev, V.; Edelman, M. The performance of current methods in ligand–protein docking. *Curr Sci.* 2002, 845-856. DOI: <https://www.jstor.org/stable/24107087>
70. Eliaa, S. G.; Al-Karmalawy, A. A.; Saleh, R. M.; Elshal, M. F. J. A. P.; Science, T. Empagliflozin and Doxorubicin Synergistically Inhibit the Survival of Triple-Negative Breast Cancer Cells via Interfering with the mTOR Pathway and Inhibition of Calmodulin: In Vitro and Molecular Docking Studies. *ACS Pharmacol. Transl. Sci.* 2020, 3, 1330-1338. DOI: <https://doi.org/10.1021/acsptsci.0c00144>
71. Abo Elmaaty, A.; Hamed, M. I. A.; Ismail, M. I.; Elkaeed, E. B.; Abulkhair, H. S.; Khattab, M.; Al-Karmalawy, A. A. Computational Insights on the Potential of Some NSAIDs for Treating COVID-19: Priority Set and Lead Optimization. *Molecules.* 2021, 26, 3772. DOI: <https://doi.org/10.3390/molecules26123772>
72. Abdallah, A. E.; Alesawy, M. S.; Eissa, S. I.; El-Fakharany, E. M.; Kalaba, M. H.; Sharaf, M. H.; Abo Shama, N. M.; Mahmoud, S. H.; Mostafa, A.; Al-Karmalawy, A. A.; Elkady, H. Design and synthesis of new 4-(2-nitrophenoxy)benzamide derivatives as potential antiviral agents: molecular modeling and in vitro antiviral screening. *New J Chem.* 2021, 45, 16557-16571. DOI: <https://doi.org/10.1039/D1NJ02710G>
73. Fasugba, O.; Mitchell, B. G.; Mnatzaganian, G.; Das, A.; Collignon, P.; Gardner, A. J. P. o. Five-year antimicrobial resistance patterns of urinary *Escherichia coli* at an Australian tertiary hospital: time series analyses of prevalence data. *PLoS One.* 2016, 11, e0164306. DOI: <https://doi.org/10.1371/journal.pone.0164306>
74. Mahi-Birjand, M.; Yaghoubi, S.; Abdollahpour-Alitappeh, M.; Keshtkaran, Z.; Bagheri, N.; Pirouzi, A.; Khatami, M.; Sineh Sepehr, K.; Peymani, P.; Karimzadeh, I. J. E. o. o. d. s. Protective effects of pharmacological agents against aminoglycoside-induced nephrotoxicity: A systematic review. *Expert Opin Drug Saf.* 2020, 19, 167-186. DOI: <https://doi.org/10.1080/14740338.2020.1712357>
75. Ali, B. H.; Al Za'abi, M.; Blunden, G.; Nemmar, A. J. B.; pharmacology, c.; toxicology. Experimental gentamicin nephrotoxicity and agents that modify it: a mini- review of recent research. *Basic Clin Pharmacol Toxicol.* 2011, 109, 225-232. DOI: <https://doi.org/10.1111/j.1742-7843.2011.00728.x>
76. Seçilmiş, M. A.; Karataş, Y.; Yorulmaz, Ö.; Büyükafşar, K.; Şingirik, E.; Doran, F.; Inal, T. C.; Dikmen, A. J. N. P. Protective effect of L-arginine intake on the impaired renal vascular responses in the gentamicin-treated rats. *Nephron Physiol.* 2005, 100, p13-p20. DOI: <https://doi.org/10.1159/000084657>
77. Rushendran, R.; Reddy, V. J.; Kumar, T. B.; Mamatha, T.; Roja, J.; Roopavani, T. J. J. o. P.-C.; Research, C. Evaluation of anti-fibrotic activity of ethanolic extract of *Nelumbo nucifera* Gaertn. Seed against doxorubicin and unilateral ureter obstruction-induced renal fibrosis. *J Pre-Clin Clin Res.* 2017, 11, 66-75. DOI: [10.26444/jpccr/75319](https://doi.org/10.26444/jpccr/75319)
78. Udupa, V.; Prakash, V. J. T. R. Gentamicin induced acute renal damage and its evaluation using urinary biomarkers in rats. *Toxicol Rep.* 2019, 6, 91-99. DOI: <https://doi.org/10.1016/j.toxrep.2018.11.015>

79. Sabra, H. A.; Ahmed, N. M. J. B. L. Reno-protective Effect of Graviola (*Annona Muricata*) Leaves Against Lead Acetate Toxicity on experimental Albino Rats. *Biochem lett.* 2018, 14, 1-13. DOI: [10.21608/BLJ.2018.47203](https://doi.org/10.21608/BLJ.2018.47203)
80. Tavafi, M.; Ahmadvand, H. J. T.; Cell. Effect of rosmarinic acid on inhibition of gentamicin induced nephrotoxicity in rats. *Tissue Cell.* 2011, 43, 392-397. DOI: <https://doi.org/10.1016/j.tice.2011.09.001>
81. Khansari, N.; Shakiba, Y.; Mahmoudi, M. J. R. p. o. i. Chronic inflammation and oxidative stress as a major cause of age-related diseases and cancer. *Recent Pat Inflamm Allergy Drug Discov.* 2009, 3, 73-80. DOI: <https://doi.org/10.2174/187221309787158371>
82. Ibrahim, M. J. A.-A. J. o. P. S. Design, synthesis, molecular docking and biological evaluation of some novel quinazoline-4 (3H)-one derivatives as anti-inflammatory agents. *Al-Azhar J Pharm Sci.* 2012, 46, 185-203. DOI: [10.21608/AJPS.2012.7145](https://doi.org/10.21608/AJPS.2012.7145)
83. Soufli, I.; Toumi, R.; Rafa, H.; Touil-Boukoffa, C. J. W. j. o. g. p. Overview of cytokines and nitric oxide involvement in immuno-pathogenesis of inflammatory bowel diseases. *World J Gastrointest Pharmacol Ther.* 2016, 7, 353. DOI: [10.4292/wjgpt.v7.i3.353](https://doi.org/10.4292/wjgpt.v7.i3.353)
84. Randjelovic, P.; Veljkovic, S.; Stojiljkovic, N.; Sokolovic, D.; Ilic, I. J. E. j. Gentamicin nephrotoxicity in animals: Current knowledge and future perspectives. *EXCLI J.* 2017, 16, 388. DOI: [10.17179/excli2017-165](https://doi.org/10.17179/excli2017-165)
85. Christo, J. S.; Rodrigues, A. M.; Mouro, M. G.; Cenedeze, M. A.; de Jesus Simões, M.; Schor, N.; Higa, E. M. S. J. N. O. Nitric oxide (NO) is associated with gentamicin (GENTA) nephrotoxicity and the renal function recovery after suspension of GENTA treatment in rats. *Nitric Oxide.* 2011, 24, 77-83. DOI: <https://doi.org/10.1016/j.niox.2010.12.001>
86. Lee, K. E.; Kim, E. Y.; Kim, C. S.; Choi, J. S.; Bae, E. H.; Ma, S. K.; Kim, K. K.; Lee, J. U.; Kim, S. W. J. B. Macrophage-stimulating protein attenuates gentamicin-induced inflammation and apoptosis in human renal proximal tubular epithelial cells. *Biochem Biophys Res Commun.* 2013, 434, 527-533. DOI: <https://doi.org/10.1016/j.bbrc.2013.03.108>
87. Abdel-Zaher, A. O.; Abdel-Rahman, M. M.; Hafez, M. M.; Omran, F. M. J. T. Role of nitric oxide and reduced glutathione in the protective effects of aminoguanidine, gadolinium chloride and oleanolic acid against acetaminophen-induced hepatic and renal damage. *Toxicol.* 2007, 234, 124-134. DOI: <https://doi.org/10.1016/j.tox.2007.02.014>
88. Pai, P. G.; Chamari Nawarathna, S.; Kulkarni, A.; Habeeba, U.; Reddy C, S.; Teerthanath, S.; Shenoy, J. P. Nephroprotective effect of ursolic acid in a murine model of gentamicin-induced renal damage. *Int Sch Res Net.* 2012. DOI: [10.5402/2012/410902](https://doi.org/10.5402/2012/410902)
89. Kandemir, F. M.; Ozkaraca, M.; Yildirim, B. A.; Hanedan, B.; Kirbas, A.; Kilic, K.; Aktas, E.; Benzer, F. J. R. f. Rutin attenuates gentamicin-induced renal damage by reducing oxidative stress, inflammation, apoptosis, and autophagy in rats. *Renal Failure.* 2015, 37, 518-525. DOI: <https://doi.org/10.3109/0886022X.2015.1006100>
90. Khan, R. A.; Khan, M. R.; Sahreen, S. J. B. c.; medicine, a. Protective effects of rutin against potassium bromate induced nephrotoxicity in rats. *BMC Complement Altern Med.* 2012, 12, 204. DOI: <https://doi.org/10.1186/1472-6882-12-204>

91. Hickey, E.; Raje, R.; Reid, V.; Gross, S.; Ray, S. Diclofenac induced in vivo nephrotoxicity may involve oxidative stress-mediated massive genomic DNA fragmentation and apoptotic cell death. *Free Radic Biol Med.* 2001, 31, 139-152. DOI: [https://doi.org/10.1016/S0891-5849\(01\)00560-3](https://doi.org/10.1016/S0891-5849(01)00560-3)
92. Kuatsienu, L. E.; Ansah, C.; Adinortey, M. B. Toxicological evaluation and protective effect of ethanolic leaf extract of *Launaea taraxacifolia* on gentamicin induced rat kidney injury. *Asian Pac J Trop Biomed.* 2017, 7, 640-646. DOI: <https://doi.org/10.1016/j.apjtb.2017.06.011>
93. Alarifi, S.; Al-Doaiss, A.; Alkahtani, S.; Al-Farraj, S.; Al-Eissa, M. S.; Al-Dahmash, B.; Al-Yahya, H.; Mubarak, M. Blood chemical changes and renal histological alterations induced by gentamicin in rats. *Saudi J Biol Sci.* 2012, 19, 103-110. DOI: <https://doi.org/10.1016/j.sjbs.2011.11.002>
94. Juan, S.-H.; Chen, C.-H.; Hsu, Y.-H.; Hou, C.-C.; Chen, T.-H.; Lin, H.; Chu, Y.-L.; Sue, Y.-M. Tetramethylpyrazine protects rat renal tubular cell apoptosis induced by gentamicin. *Nephrol Dial Transplant.* 2007, 22, 732-739. DOI: <https://doi.org/10.1093/ndt/gfl699>
95. Abdelrahman, R. S.; Abdelmageed, M. E. Renoprotective effect of celecoxib against gentamicin-induced nephrotoxicity through suppressing NFκB and caspase-3 signaling pathways in rats. *Chem Biol Interact.* 2020, 315, 108863. DOI: <https://doi.org/10.1016/j.cbi.2019.108863>
96. Sano, R.; Reed, J. C. ER stress-induced cell death mechanisms. *Biochim Biophys Acta Mol Cell Res.* 2013, 1833, 3460-3470. DOI: <https://doi.org/10.1016/j.bbamcr.2013.06.028>
97. Ali, H. J. T. M. R. Evaluation of antioxidants effect of *Citrus reticulata* in *Schistosoma mansoni* infected mice. *Trends Med Res.* 2007, 2, 37-43. DOI: [10.3923/tmr.2007.37.43](https://doi.org/10.3923/tmr.2007.37.43)
98. Hajihashemi, S.; Ahmadi, M.; Chehrei, A.; Ghanbari, F. J. A. J. o. P. Ameliorative effect of cotreatment with the methanolic leaf extract of *Urtica dioica* on acute kidney injury induced by gentamicin in rats. *Avicenna J Phytomed.* 2020, 10, 273. PMID: [32523882](https://pubmed.ncbi.nlm.nih.gov/32523882/)
99. Alm-Eldeen, A. A.; El-Naggar, S. A.; El-Boray, K. F.; Elgebaly, H. A.; Osman, I. H. J. T. J. o. P. R. Protective role of *Commiphora molmol* extract against liver and kidney toxicity induced by carbon tetrachloride in mice. *Trop J Pharm Res.* 2016, 15, 65-72. DOI: [10.4314/tjpr.v15i1.9](https://doi.org/10.4314/tjpr.v15i1.9)
100. Abdel-Daim, M. M.; Ghazy, E. W.; Fayez, M. Synergistic protective role of mirazid (*Commiphora molmol*) and ascorbic acid against tilmicosin-induced cardiotoxicity in mice. *Can J Physiol Pharmacol.* 2015, 93, 45-51. DOI: <https://doi.org/10.1139/cjpp-2014-0336>
101. Al-Harbi, M.; Qureshi, S.; Raza, M.; Ahmed, M.; Afzal, M.; Shah, A. Gastric antiulcer and cytoprotective effect of *Commiphora molmol* in rats. *J Ethnopharmacol.* 1997, 55, 141-150. DOI: [https://doi.org/10.1016/S0378-8741\(96\)01488-2](https://doi.org/10.1016/S0378-8741(96)01488-2)
102. Abdelrahman, R. Protective effect of apocynin against gentamicin-induced nephrotoxicity in rats. *Hum Exp Toxicol.* 2018, 37, 27-37. DOI: <https://doi.org/10.1177/0960327116689716>
103. Gill, S. S.; Tuteja, N. J. Reactive oxygen species and antioxidant machinery in abiotic stress tolerance in crop plants. *Plant Physiol Biochem.* 2010, 48, 909-930. DOI: <https://doi.org/10.1016/j.plaphy.2010.08.016>



104. Hamed, M. A.; Hetta, M. H. Efficacy of *Citrus reticulata* and Mirazid in treatment of *Schistosoma mansoni*. *Mem Inst Oswaldo Cruz*. 2005, 100, 771-778. DOI: [10.1590/s0074-02762005000700017](https://doi.org/10.1590/s0074-02762005000700017)
105. Yang, M.; Chen, J.; Zhao, J.; Meng, M. Etanercept attenuates myocardial ischemia/reperfusion injury by decreasing inflammation and oxidative stress. *PLoS One*. 2014, 9, e108024. DOI: <https://doi.org/10.1371/journal.pone.0108024>
106. Jaikumkao, K.; Pongchaidecha, A.; Thongnak, L.-o.; Wanchai, K.; Arjinajarn, P.; Chatsudthipong, V.; Chattipakorn, N.; Lungkaphin, A. Amelioration of renal inflammation, endoplasmic reticulum stress and apoptosis underlies the protective effect of low dosage of atorvastatin in gentamicin-induced nephrotoxicity. *PLoS One*. 2016, 11, e0164528. DOI: <https://doi.org/10.1371/journal.pone.0164528>
107. Kim, S. Y.; Moon, A. J. B. Drug-induced nephrotoxicity and its biomarkers. *Biomol Ther*. 2012, 20, 268. DOI: [10.4062/biomolther.2012.20.3.268](https://doi.org/10.4062/biomolther.2012.20.3.268)
108. Cassidy, H.; Radford, R.; Slyne, J.; O'Connell, S.; Slattery, C.; Ryan, M. P.; McMorrow, T. The role of MAPK in drug-induced kidney injury. *J Signal Trans*. 2012, 2012. DOI: [10.1155/2012/463617](https://doi.org/10.1155/2012/463617)
109. Grynberg, K.; Ma, F. Y.; Nikolic-Paterson, D. J. The JNK signaling pathway in renal fibrosis. *Front Physiol*. 2017, 8, 829. DOI: <https://doi.org/10.3389/fphys.2017.00829>
110. Saleh, M. A.; Antar, S. A.; Hazem, R. M.; El-Azab, M. F. Pirfenidone and Vitamin D Ameliorate Cardiac Fibrosis Induced by Doxorubicin in Ehrlich Ascites Carcinoma Bearing Mice: Modulation of Monocyte Chemoattractant Protein-1 and Jun N-terminal Kinase-1 Pathways. *Pharmaceuticals*. 2020, 13, 348. DOI: <https://doi.org/10.3390/ph13110348>
111. Morikawa, T.; Matsuda, H.; Yoshikawa, M. A review of anti-inflammatory terpenoids from the incense gum resins frankincense and myrrh. *J Oleo Sci*. 2017, ess16149. DOI: <https://doi.org/10.5650/jos.ess16149>
112. Nakanishi, H.; Kaibori, M.; Teshima, S.; Yoshida, H.; Kwon, A.-H.; Kamiyama, Y.; Nishizawa, M.; Ito, S.; Okumura, T. Pirfenidone inhibits the induction of iNOS stimulated by interleukin-1 $\beta$  at a step of NF- $\kappa$ B DNA binding in hepatocytes. *J Hepatol*. 2004, 41, 730-736. DOI: <https://doi.org/10.1016/j.jhep.2004.07.007>
113. Christian, F.; Smith, E. L.; Carmody, R. J. The regulation of NF- $\kappa$ B subunits by phosphorylation. *Cells*. 2016, 5, 12. DOI: <https://doi.org/10.3390/cells5010012>
114. Rao, Y. K.; Fang, S.-H.; Tzeng, Y.-M. Anti-inflammatory activities of flavonoids isolated from *Caesalpinia pulcherrima*. *J Ethnopharmacol*. 2005, 100, 249-253. DOI: <https://doi.org/10.1016/j.jep.2005.02.039>